

Supplementary for “Imaging surface plasmons: the fingerprint of leaky waves on the far field”

Aurélien Drezet, Cyriaque Genet
*Institut Néel UPR 2940, CNRS-University Joseph Fourier,
 25 rue des Martyrs, 38000 Grenoble, France and
 Laboratoire des Nanostructures, ISIS, Université de Strasbourg,
 CNRS (UMR7006) 8 allée Gaspard Monge, 67000 Strasbourg, France*
 (Dated: February 24, 2014)

PACS numbers: 42.25.Lc, 42.70.-a, 73.20.Mf

I. INTRODUCTION

We start with a scalar potentials expansion of the electromagnetic field in the three media $j = 1, 2, 3$ corresponding respectively to air metal and substrate (i.e. glass or fused silica). There is no source in the substrate and the dipole (point source) is located in medium $j = 1$. We write for the field in each medium:

$$\begin{aligned}\mathbf{D}_j &= \nabla \times \nabla \times [\hat{\mathbf{z}}\Psi_{\text{TM},j}] + ik_0\varepsilon_j \nabla \times [\hat{\mathbf{z}}\Psi_{\text{TE},j}] \\ \mathbf{B}_j &= \nabla \times \nabla \times [\hat{\mathbf{z}}\Psi_{\text{TE},j}] - ik_0 \nabla \times [\hat{\mathbf{z}}\Psi_{\text{TM},j}]\end{aligned}\quad (1)$$

with

$$[\nabla^2 + k_0^2\varepsilon_j]\Psi_{\text{TM,TE},j} = 0. \quad (2)$$

Using Boundary conditions we show that the only non vanishing scalar potentials for the dipole direction perpendicular to the film is in medium $j = 3$

$$\begin{aligned}\Psi^{\text{TM},\perp}(\mathbf{x}, z) &= \frac{i\mu_{\perp}}{4\pi} \int_0^{+\infty} \frac{kdk}{k_1} \tilde{T}_{13}^{\text{TM}}(k) e^{ik_1h} e^{ik_3z} J_0(k\rho) \\ &= \frac{i\mu_{\perp}}{8\pi} \int_{-\infty}^{+\infty} \frac{kdk}{k_1} \tilde{T}_{13}^{\text{TM}}(k) e^{ik_1h} e^{ik_3z} H_0^{(+)}(k\rho),\end{aligned}\quad (3)$$

where we defined $k_i = \sqrt{k_0^2\varepsilon_i - k^2}$ with $\text{Imag}[k_j] \geq 0$, $k_0 = 2\pi/\lambda = \omega/c$, and $z \geq d$. To obtain Eq. 3 we also used the formula $H_0^{(+)}(u) - H_0^{(+)}(-u) = 2J_0(u)$ which is valid in the complex plane $u = u' + iu''$ (if $|\arg(z)| < \pi$). The Fresnel coefficient characterizing the transmission of the metal film is for TM waves defined by

$$\tilde{T}_{13}^{\text{TM}}(k) = \frac{T_{23}^{\text{TM}}T_{12}^{\text{TM}}}{1 + R_{23}^{\text{TM}}R_{12}^{\text{TM}}e^{2ik_2d}} e^{i(k_2-k_3)d} \quad (4)$$

where

$$R_{ij}^{\text{TM}} = \frac{k_i/\varepsilon_i - k_j/\varepsilon_j}{k_i/\varepsilon_i + k_j/\varepsilon_j} \quad (5)$$

$$T_{ij}^{\text{TM}} = \frac{2k_i/\varepsilon_i}{k_i/\varepsilon_i + k_j/\varepsilon_j}. \quad (6)$$

We then introduce the variables $k = k_0n \sin \xi$, $k_3 = k_0n \cos \xi$ with $\xi = \xi' + i\xi''$ and write

$$\Psi^{\text{TM},\perp}(\mathbf{x}, z) = \int_{\Gamma} d\xi F_+^{\text{TM},\perp}(\xi) e^{ik_0n((z-d)\cos \xi + \rho \sin \xi)} \quad (7)$$

with

$$\begin{aligned}F_+^{\text{TM},\perp}(\xi) &= \frac{i\mu_{\perp}}{8\pi} \frac{k_0n \sin \xi \cos \xi}{\sqrt{(\frac{\varepsilon_1}{\varepsilon_3} - \sin^2 \xi)}} \tilde{T}_{13}^{\text{TM}}(k_0n \sin \xi) \\ &e^{i\sqrt{(\frac{\varepsilon_1}{\varepsilon_3} - \sin^2 \xi)}h} \cdot e^{ik_0nd \cos \xi} H_0^{(+)}(k_0n\rho \sin \xi) e^{-ik_0n\rho \sin \xi}\end{aligned}\quad (8)$$

(we point out that the ϱ and φ dependencies are here and in the following implicit in our notation: $F_+(\xi) := F_+(\xi, \varphi, \varrho)$). Similar expressions can be obtained for the components $\boldsymbol{\mu}_{||}$ of the dipole parallel to the interface. More precisely for the TM modes we have

$$\Psi^{\text{TM},||}(\mathbf{x}, z) = \int_{\Gamma} d\xi F_+^{\text{TM},||}(\xi) e^{ik_0 n((z-d) \cos \xi + \varrho \sin \xi)} \quad (9)$$

with

$$F_+^{\text{TM},||}(\xi) = \frac{\boldsymbol{\mu}_{||} \cdot \hat{\boldsymbol{\rho}}}{8\pi} k_0 n \cos \xi \tilde{T}_{13}^{\text{TM}}(k_0 n \sin \xi) e^{i\sqrt{(\frac{\varepsilon_1}{\varepsilon_3} - \sin^2 \xi)h}} \cdot e^{ik_0 n d \cos \xi} H_1^{(+)}(k_0 n \varrho \sin \xi) e^{-ik_0 n \varrho \sin \xi}. \quad (10)$$

Similarly for the TE waves we obtain:

$$\Psi^{\text{TE},||}(\mathbf{x}, z) = \int_{\Gamma} d\xi F_+^{\text{TE},||}(\xi) e^{ik_0 n((z-d) \cos \xi + \varrho \sin \xi)} \quad (11)$$

with

$$F_+^{\text{TE},||}(\xi) = -\frac{\boldsymbol{\mu}_{||} \cdot \hat{\boldsymbol{\varphi}}}{8\pi} \frac{k_0 \cos \xi}{\sqrt{(\frac{\varepsilon_1}{\varepsilon_3} - \sin^2 \xi)}} \tilde{T}_{13}^{\text{TE}}(k_0 n \sin \xi) e^{i\sqrt{(\frac{\varepsilon_1}{\varepsilon_3} - \sin^2 \xi)h}} \cdot e^{ik_0 n d \cos \xi} H_1^{(+)}(k_0 n \varrho \sin \xi) e^{-ik_0 n \varrho \sin \xi}. \quad (12)$$

We used the formula $H_1^{(+)}(u) + H_1^{(+)}(-u) = 2J_1(u)$. Here the Fresnel coefficients are defined by

$$\tilde{T}_{13}^{\text{TE}}(k) = \frac{T_{23}^{\text{TE}} T_{12}^{\text{TE}}}{1 + R_{23}^{\text{TE}} R_{12}^{\text{TE}} e^{2ik_2 d}} e^{i(k_2 - k_3)d} \quad (13)$$

with

$$R_{ij}^{\text{TE}} = \frac{k_i - k_j}{k_i + k_j} \quad (14)$$

$$T_{ij}^{\text{TE}} = \frac{2k_i}{k_i + k_j}. \quad (15)$$

The presence of the singular Hankel functions $H_1^{(+)}$ and $H_0^{(+)}$ in all these expressions imply the existence of a branch cut starting at the origin and associated with the function $1/\sqrt{(\sin \xi)}$. This branch cut is chosen in order to have no influence during subsequent contour deformations and is running just below the actual path Γ slightly off the real axis ξ' and to the left of the vertical line $\xi'' = -\pi/2$ (the original branch cut is composed of the line $\xi' = -\pi/2$ and of the half-axis $[\xi'' = 0, \xi' \leq 0]$). We also introduce the polar coordinates $\varrho = r \sin \vartheta$, $z = d + r \cos \vartheta$ leading to $(z - d) \cos \xi + \varrho \sin \xi = r \cos(\xi - \vartheta)$ and therefore:

$$\Psi(\mathbf{x}, z) = \int_{\Gamma} d\xi F_+(\xi) e^{ik_0 n r \cos(\xi - \vartheta)}. \quad (16)$$

The definition of the square root $k_1 = k_0 n \sqrt{(\frac{\varepsilon_1}{\varepsilon_3} - \sin^2 \xi)}$, with $\varepsilon_3 = n^2$ real and $\varepsilon_1 = \varepsilon'_1 + i\varepsilon''_1 \sim 1 + i\delta$ with $\delta \rightarrow 0^+$, implies the presence of a branch cut which must be chosen carefully in order i) to be consistent with the choice for k_1 made in Eq. 3 during integration along the contour Γ , ii) to allow further contour deformations leading to convergent calculations. The branch cut adapted to our problem is shown in Figs. 1,2 and correspond to the choice $\text{Imag}[k_1] \geq 0$ in the whole complex ξ -plane. The branch cut starts at the branch point M of coordinate ξ_c defined by the condition $k_1 = 0$. We point out that due to invariance of the Fresnel coefficient $\tilde{T}_{13}^{\text{TM},\text{TE}}(k_0 n \sin \xi)$ over the permutation $k_2 \leftrightarrow -k_2$ we don't actually need an additional branch cut for k_2 (this important property will survive for a larger number of layers).

II. THE DIFFERENT CONTRIBUTIONS ALONG THE CLOSED CONTOUR

After introducing the function $f(\xi) = i \cos(\xi - \vartheta) = i \cos(\xi' - \vartheta) \cosh \xi'' + \sin(\xi' - \vartheta) \sinh \xi''$ we define the steepest descent path SDP by the condition

$$\text{Imag}[f(\xi)] = \cos(\xi' - \vartheta) \cosh \xi'' = 1. \quad (17)$$

SDP goes through the saddle point ξ_0 defined by the condition $\frac{df(\xi)}{d\xi} = 0$ which has a solution at $\xi_0 = \vartheta$. Importantly, there are actually two trajectories solutions of Eq. 17 and going through ξ_0 . We choose the one such that the real part of $f(\xi)$ decay uniformly along SDP when going away arbitrarily to the left or to the right from the saddle point (see Fig. 1).

Cauchy theorem allows us to deform the original Γ contour to include SDP as a part of the integration path. For this we label Γ by the letter $ABCD$ (see Fig. 1). The integral in Eq. 16 is thus written $\int_{\Gamma} = \int_{ABCD}$. We will consider two cases depending whether ϑ is or not larger than the real part of the branch point $\xi'_c \simeq \arcsin(1/n) = \vartheta_c$.

A. Closing the contour in the case $\vartheta > \xi'_c$

If $\vartheta > \xi'_c$ the closed integration contour contain eight contributions (see Fig. 1) and we have:

$$0 = \int_{\Gamma} + \int_{DE} + \int_{EF} + \int_{FG} + \int_{GH} + \int_{HI} + \int_{IA} - I_{SP}. \quad (18)$$

The contribution

$$\begin{aligned} \int_{DE} &:= \int_{DE} d\xi F_+(\xi) e^{ik_0 n r \cos(\xi - \vartheta)} \\ &= \int_{\pi/2 - i\infty}^{\pi/2 + \vartheta - i\infty} d\xi F_+(\xi) e^{ik_0 n r \cos(\xi - \vartheta)} \end{aligned} \quad (19)$$

approaches zero asymptotically and can therefore be neglected.

Similarly, we can neglect $\int_{IA} := \int_{+i\infty}^{-\pi/2 + i\infty} d\xi F_+(\xi) e^{ik_0 n r \cos(\xi - \vartheta)}$ which approaches also zero asymptotically.

The contribution \int_{EF} and \int_{FG} are calculated along the SDP . However, due to the presence of the branch cut crossing SDP at F the integration along FG actually corresponds to a change of Riemann sheet associated with the second determination for the square root k_1 (we point out that since the branch cut is very close to the imaginary axis at F we have at the limit $\xi_F \simeq i \text{arccosh}(1/\cos \vartheta)$). More precisely if we call “+” the Riemann sheet in which $\text{Imag}[k_1] \geq 0$ the second Riemann surface “-” associated with the condition $\text{Imag}[k_1] \leq 0$ is connected to “+” through the branch cut represented in Fig. 1. Therefore, crossing the branch cut at F corresponds actually to a change in sign of the square root $k_1 \rightarrow -k_1$. We have consequently the contributions

$$\begin{aligned} \int_{EF} &:= \int_{EF} d\xi F_+(\xi) e^{ik_0 n r \cos(\xi - \vartheta)} \\ \int_{FG} &:= \int_{FG} d\xi F_-(\xi) e^{ik_0 n r \cos(\xi - \vartheta)} \end{aligned} \quad (20)$$

where $F_-(\xi)$ is the same function of k as $F_+(\xi)$ but $\sqrt{(\frac{\varepsilon_1}{\varepsilon_3} - \sin^2 \xi)}$ (defined with $\text{Imag}[\sqrt{(\frac{\varepsilon_1}{\varepsilon_3} - \sin^2 \xi)}] \geq 0$) is now replaced by $-\sqrt{(\frac{\varepsilon_1}{\varepsilon_3} - \sin^2 \xi)}$. More precisely the square root $z_+ = \sqrt{g}$ of the complex variable $g' + ig''$ is defined on the “+” Riemann sheet by $z_+ = \text{sign}(g'') \sqrt{((g' + |g|)/2)} + i \sqrt{((-g' + |g|)/2)}$ where $\text{sign}(x) = 1$ if $x > 0$, $\text{sign}(x) = -1$ if $x < 0$ and $\text{sign}(x) = 0$ if $x = 0$. On the “-” sheet we have therefore $z_- = -z_+$. An important remark concerns here the integration convergence along the SDP when approaching the vertical asymptotes $\pm \frac{\pi}{2} + \vartheta \mp i\infty$. Indeed, due to the presence of the coefficient $e^{\pm ik_0 n h \sqrt{(\frac{\varepsilon_1}{\varepsilon_3} - \sin^2 \xi)}}$ in the definition of $F_{\pm}(\xi)$ it is not obvious that the integrand will take a finite value at infinity. Actually a careful study of the limit behaviour of $F_{\pm}(\xi)$ including the exponentials terms as well as the Hankel function contribution shows that there is no convergence problem for $F_+(\xi)$ at infinity (this also explains why \int_{DE} and \int_{IA} goes to zero asymptotically). However when going on the “-” Riemann sheet the convergence is not always ensured. We found that however no problem occurs on this second sheet as soon as

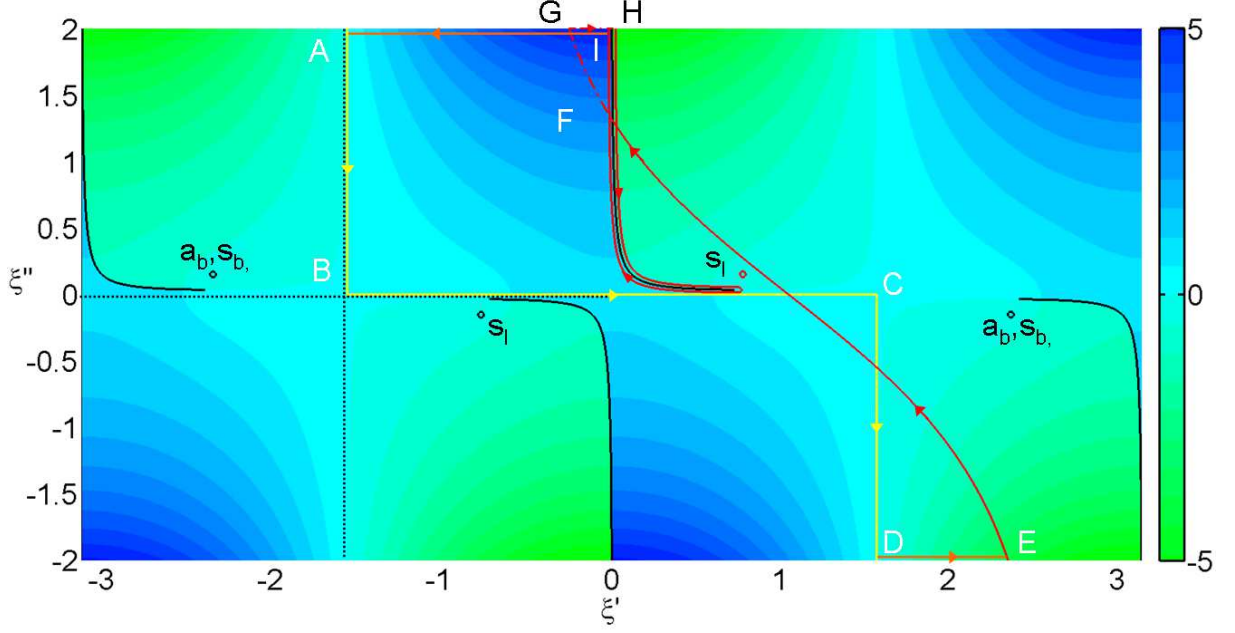


FIG. 1: Integration contour in the complex ξ -plane for $\vartheta > \xi'_c$.

the condition $z + \varrho \tan \vartheta > h$ is verified. In particular, no problem appears if we impose $z > h$. Since here we are interested in the asymptotic behavior valid for $z \gg h$ this condition will be automatically satisfied.

This point is particularly relevant when we consider the contribution $\tilde{f}_{GH} := \int_{-\pi/2+\vartheta+i\infty}^{i\infty} d\xi F_-(\xi) e^{ik_0 n r \cos(\xi-\vartheta)}$ which approaches zero if the previous condition $z > h$ is fulfilled. From H we thus cross the branch cut and go back to the “+” sheet. We thus obtain a contour $\int_{HI} = \int_{HI} d\xi F_+(\xi) e^{ik_0 n r \cos(\xi-\vartheta)}$ longing the branch cut in the original “+” space and contouring the branch point $k_1 = 0$ (corresponding nearly to $\xi_c \simeq \arcsin(1/n) = \vartheta_c$). We will see in the subsection D that this contribution corresponds to a lateral wave associated with a Goos-Hänchen effect in transmission.

Finally, due to the presence of isolated singularities in the complex plane (i.e. poles) for the TM waves we must subtract a residue contribution I_{SP} which value will precisely depends on the position ϑ along the real axis (i.e. whether or not the poles are encircled by the closed contour in the complex ξ -plane). A complete analysis of these singularities show that we can in principle extract from the transmission coefficient $\tilde{T}_{13}^{\text{TM}}(k)$ four poles corresponding to the four SP modes guided along the metal slab. However, the branch cut choice made here allows only the existence of three solutions called respectively symmetric leaky (s_l), symmetric bound (s_b) and asymmetric bound (a_b) modes. The two bound modes are always well outside the region of integration and are never encircled by the contour. Only the leaky mode s_l can eventually contribute as a residue depending whether or not the angle ϑ is larger than the leakage radiation angle ϑ_{LR} defined by the condition $\cos(\xi'_p - \vartheta_{LR}) \cosh \xi''_p = 1$ (with ξ_p the complex coordinate of the SP pole s_l). This implies:

$$\vartheta_{LR} = \xi'_p + \arccos(1/\cosh \xi''_p) \simeq \xi'_p, \quad (21)$$

and therefore the residue contribution is written:

$$I_{SP} = 2\pi i \text{Res}[F_+(\xi_p)] e^{ik_0 n r \cos(\xi_p - \vartheta)} \Theta(\vartheta - \vartheta_{LR}). \quad (22)$$

In the following we write $k_p = k_0 n \sin \xi_p$, $k_{3,p} = k_0 n \cos \xi_p$ and $k_{1,p} = k_0 n \sqrt{(\frac{\varepsilon_1}{\varepsilon_3} - \sin^2 \xi_p)}$ the pole wavevectors associated with this s_l mode. The calculation of the different residues is straightforward and leads for the vertical dipole case to:

$$\text{Res}[F_+^{\text{TM},\perp}(\xi_p)] e^{ik_0 n r \cos(\xi_p - \vartheta)} = \frac{i\mu_{\perp}}{8\pi} \frac{k_0 n \sin \xi_p \cos \xi_p}{\sqrt{(\frac{\varepsilon_1}{\varepsilon_3} - \sin^2 \xi_p)}} \text{Res}[\tilde{T}_{13}^{\text{TM}}(k_0 n \sin \xi_p)] e^{i\sqrt{(\frac{\varepsilon_1}{\varepsilon_3} - \sin^2 \xi_p)h}} \cdot e^{ik_0 n z \cos \xi_p} H_0^{(+)}(k_0 n \varrho \sin \xi_p) \quad (23)$$

We now write $\tilde{T}_{13}^{\text{TM}}(k)$ as a rational fraction $\frac{N_{13}(k)}{D_{13}(k)}$ (with polynomial functions $N_{13}(k)$, $D_{13}(k)$ of the variable k) and therefore for the single pole ξ_p we get

$$\text{Res}[\tilde{T}_{13}^{\text{TM}}(k_0 n \sin \xi_p)] = \frac{N_{13}(k_p)}{\frac{\partial D_{13}(k_0 n \sin \xi_p)}{\partial \xi_p}} = \frac{1}{k_{3,p}} \frac{N_{13}(k_p)}{\frac{\partial D_{13}(k_p)}{\partial k_p}}.$$

We thus have finally

$$\begin{aligned} & \text{Res}[F_+^{\text{TM},\perp}(\xi_p)] e^{ik_0 n r \cos(\xi_p - \vartheta)} \\ &= \frac{i\mu_{\perp}}{8\pi} \frac{k_p}{k_{1,p}} e^{ik_{1,p}h} e^{ik_{3,p}z} \frac{N_{13}(k_p)}{\frac{\partial D_{13}(k_p)}{\partial k_p}} H_0^{(+)}(k_p \varrho). \end{aligned} \quad (24)$$

A similar expression is obtained for the horizontal dipole:

$$\begin{aligned} & \text{Res}[F_+^{\text{TM},\parallel}(\xi_p)] e^{ik_0 n r \cos(\xi_p - \vartheta)} \\ &= \frac{\mu_{\parallel} \cdot \hat{\boldsymbol{\varrho}}}{8\pi} e^{ik_{1,p}h} e^{ik_{3,p}z} \frac{N_{13}(k_p)}{\frac{\partial D_{13}(k_p)}{\partial k_p}} H_1^{(+)}(k_p \varrho). \end{aligned} \quad (25)$$

There is no residue for the TE modes.

Going back to the SDP contribution we define the variable $\tau = e^{i\pi/4} \sqrt{2} \sin((\xi - \vartheta)/2)$ which leads to $f(\xi) = i - \tau^2$. Along SDP τ is real such that $\tau^2 = -\sin(\xi' - \vartheta) \sinh \xi'' \geq 0$. We thus obtain $\tau = 2 \sin((\xi' - \vartheta)/2) \cosh(\xi''/2)$. The saddle point corresponds to $\tau = 0$ ($\tau > 0$ if $\xi'' < 0$ and $\tau < 0$ if $\xi'' > 0$ along SDP). With this new variable the point F has therefore the coordinate $\tau_F \simeq -2 \sin(\vartheta/2) \cosh(\frac{1}{2} \text{arccosh}(1/\cos(\vartheta))) = -2 \sin(\vartheta/2) \sqrt{1 + \frac{1}{\cos \vartheta}} < 0$. Defining the term $I_{SDP} = -\int_{EF} - \int_{FG}^{\sim}$ we therefore obtain

$$\begin{aligned} I_{SDP} &= e^{ik_0 n r} \left\{ \int_{-\infty}^{\tau_F^-} d\tau G_-(\tau) e^{-k_0 n r \tau^2} \right. \\ &\quad \left. + \int_{\tau_F^+}^{+\infty} d\tau G_+(\tau) e^{-k_0 n r \tau^2} \right\} \\ &= e^{ik_0 n r} \int_{-\infty}^{+\infty} d\tau \{ G_+(\tau) [1 - \Theta(\tau_F - \tau)] \\ &\quad + G_-(\tau) [1 - \Theta(\tau - \tau_F)] \} e^{-k_0 n r \tau^2} \end{aligned} \quad (26)$$

where we defined $G_{\pm}(\tau) = F_{\pm}(\xi) \frac{d\xi}{d\tau}$ and used $\frac{d\xi}{d\tau} = \sqrt{2} e^{-i\pi/4} / \cos((\xi - \vartheta)/2)$. We introduced the Heaviside step function $\Theta(x)$ defined as: $\Theta(x) = 1$ if $x \geq 0$ and $\Theta(x) = 0$ otherwise. Importantly $\lim_{\tau \rightarrow \tau_F^+} G_+(\tau) = \lim_{\tau \rightarrow \tau_F^-} G_-(\tau)$ and therefore the function $G(\tau) = G_+(\tau)(1 - \Theta(\tau_F - \tau)) + G_-(\tau)(1 - \Theta(\tau - \tau_F))$ which is not defined at τ_F can be prolonged without difficulties at F .

B. Closing the contour in the case $\vartheta < \xi'_c$

If $\vartheta < \xi'_c$ the closed integration contour contain 6 contributions (see Fig. 2) and we have:

$$0 = \int_{\Gamma} + \int_{DE} + \int_{EF} + \int_{FG}^{\sim} + \int_{GH} + \int_{HA}. \quad (27)$$

All these contribution but \int_{NM} are defined on the “+” Riemann sheet. \int_{HA} and \int_{DE} tends asymptotically to zero for reasons already discussed in the previous paragraph. Importantly there is no contribution along the branch cut since the integration path along SDP starts and finishes on the proper Riemann sheet “+”. Regrouping the terms we thus have for $\vartheta > \xi'_c$: $\int_{\Gamma} = I_{SDP} = -\int_{EF} - \int_{FG}^{\sim} - \int_{GH}$ with

$$\begin{aligned} \int_{EF} &:= \int_{EF} d\xi F_+(\xi) e^{ik_0 n r \cos(\xi - \vartheta)} \\ \int_{FG}^{\sim} &:= \int_{FG} d\xi F_-(\xi) e^{ik_0 n r \cos(\xi - \vartheta)} \\ \int_{GH} &:= \int_{GH} d\xi F_+(\xi) e^{ik_0 n r \cos(\xi - \vartheta)}. \end{aligned} \quad (28)$$

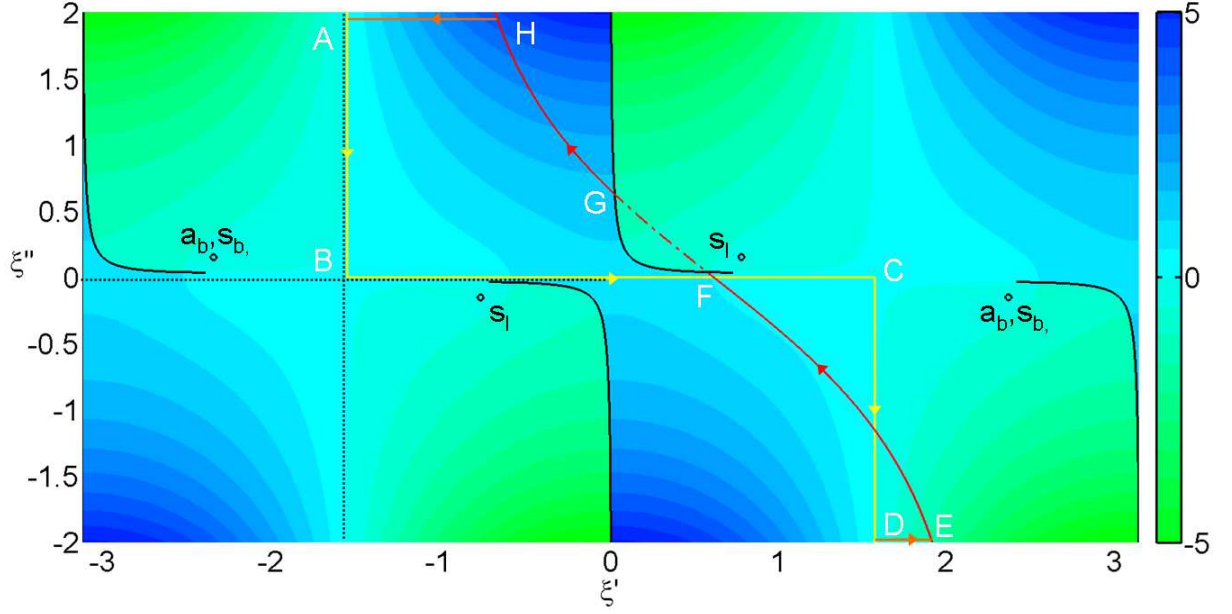


FIG. 2: Integration contour in the complex ξ -plane for $\vartheta < \xi'_c$.

We then use the same variable τ and function $G_{\pm}(\tau)$ and thus obtain

$$\begin{aligned}
 I_{SDP} = e^{ik_0 nr} \{ & \int_{-\infty}^{\tau_F^-} d\tau G_+(\tau) e^{-k_0 nr \tau^2} \\
 & + \int_{\tau_F^+}^{\tau_G^-} d\tau G_+(\tau) e^{-k_0 nr \tau^2} \\
 & + \int_{\tau_G^+}^{-\infty} d\tau G_+(\tau) e^{-k_0 nr \tau^2} \}
 \end{aligned} \tag{29}$$

which is rewritten as

$$I_{SDP} = e^{ik_0 nr} \int_{-\infty}^{\tau_F^-} d\tau G(\tau) e^{-k_0 nr \tau^2} \tag{30}$$

with

$$\begin{aligned}
 G(s) = & G_+(\tau)[1 - \Theta(\tau - \tau_F)] \\
 & + G_+(\tau)[1 - \Theta(\tau_G - \tau)] \\
 & + G_-(\tau)[1 - \Theta(\tau_F - \tau)][1 - \Theta(\tau - \tau_G)].
 \end{aligned} \tag{31}$$

C. The Steepest descent path contribution

The previous integral I_{SDP} for both $\vartheta > \xi'_c$ and $\vartheta < \xi'_c$ is of the gaussian form and can be evaluated by doing a Taylor expansion of $G(\tau)$ around $\tau = 0$. Using well known integrals we thus obtain

$$I_{SDP} = e^{ik_0 nr} \sum_{m \in \text{even}} \frac{\Gamma(\frac{m+1}{2})}{m! (k_0 nr)^{\frac{m+1}{2}}} \frac{d^m}{d\tau^m} G(0). \tag{32}$$

It is important to observe that $G(\tau)$ is highly singular in the vicinity of the SP pole s_l . Writing τ_p the coordinate of the pole in the τ -space we thus define

$$G(\tau) := G_0(\tau) + \frac{\text{Res}[G(\tau_p)]}{\tau - \tau_p} \tag{33}$$

which (together with Eq. 32) immediately implies

$$I_{SDP} = e^{ik_0 nr} \sum_{m \in \text{even}} \frac{\Gamma(\frac{m+1}{2})}{(k_0 nr)^{\frac{m+1}{2}}} \left\{ \frac{1}{m!} \frac{d^m}{d\tau^m} G_0(0) - \frac{\text{Res}[G(\tau_p)]}{\tau_p^{m+1}} \right\}. \quad (34)$$

Remarkably, the singular integral

$$I_{SDP}^{\text{pole}} := e^{ik_0 nr} \int_{-\infty}^{+\infty} d\tau \frac{\text{Res}[G(\tau_p)]}{\tau - \tau_p} e^{-k_0 nr \tau^2}$$

can be directly calculated and we thus obtain

$$I_{SDP} = e^{ik_0 nr} \sum_{m \in \text{even}} \frac{\Gamma(\frac{m+1}{2})}{m! (k_0 nr)^{\frac{m+1}{2}}} \frac{d^m}{d\tau^m} G_0(0) + I_{SDP}^{\text{pole}} \quad (35)$$

with

$$\begin{aligned} I_{SDP}^{\text{pole}} &= -2i\pi \text{Res}[G(\tau_p)] e^{ik_0 nr \cos(\xi_p - \vartheta)} \left\{ \Theta(-\tau_p'') - \frac{1}{2} \text{erfc}(-i\tau_p \sqrt{(k_0 nr)}) \right\} \\ &= -e^{ik_0 nr} \sum_{m \in \text{even}} \frac{\Gamma(\frac{m+1}{2})}{(k_0 nr)^{\frac{m+1}{2}}} \frac{\text{Res}[G(\tau_p)]}{\tau_p^{m+1}} \end{aligned} \quad (36)$$

where $\text{erfc}(z) = (2/\sqrt{\pi}) \int_z^{+\infty} e^{-t^2} dt$ is the Gauss complementary error function. Notably, we have (see appendix) $\text{Res}[G(\tau_p)] = \text{Res}[F_+(\xi_p)]$ and $\Theta(-\tau_p'') = \Theta(\vartheta - \vartheta_{LR})$ therefore I_{SDP}^{pole} contains up to the sign difference the same contribution which already appeared in I_{SP} . Consequently, the sum $I_{SDP}^{\text{pole}} + I_{SP}$ of the two contributions proportional to the residue represents a simple explicit mathematical expression:

$$\begin{aligned} &I_{SDP}^{\text{pole}} + I_{SP} \\ &= i\pi \text{Res}[G(\tau_p)] e^{ik_0 nr \cos(\xi_p - \vartheta)} \text{erfc}(-i\tau_p \sqrt{(k_0 nr)}). \end{aligned} \quad (37)$$

This sum is sometimes by definition associated with the surface plasmon mode. We point out however that the error function is highly singular and therefore we should preferably use the equivalent expression:

$$\begin{aligned} I_{SDP}^{\text{pole}} + I_{SP} &= 2i\pi \text{Res}[G(\tau_p)] e^{ik_0 nr \cos(\xi_p - \vartheta)} \Theta(\vartheta - \vartheta_{LR}) \\ &\quad - e^{ik_0 nr} \sum_{m \in \text{even}} \frac{\Gamma(\frac{m+1}{2})}{(k_0 nr)^{\frac{m+1}{2}}} \frac{\text{Res}[G(\tau_p)]}{\tau_p^{m+1}}. \end{aligned} \quad (38)$$

We also note that most of the discussions and confusions made during the XXth on the role of SPs in the Sommerfeld integral resulted from the above mentioned intricate relationship existing between the two singular terms I_{SP} and I_{SDP}^{pole} . For a historical discussion see Collin[1].

D. The lateral wave contribution: Goos-Hänchen effect in transmission

In the case $\vartheta > \xi'_c$ the integral \int_{HI} along the branch cut can be transformed using the method described in Ref. 2. For this we separate the integral $\int_{HI} d\xi F_+(\xi) e^{ik_0 nr \cos(\xi - \vartheta)}$ into a contribution $\int_{HM} = \int_{HM} d\xi F_+(\xi) e^{ik_0 nr \cos(\xi - \vartheta)}$ starting at infinity at $\xi = i\infty + 0^+$ and stopping at the branch-point M ($\xi_c \simeq \vartheta_c$) and into a contribution $\int_{MI} = \int_{MI} d\xi F_+(\xi) e^{ik_0 nr \cos(\xi - \vartheta)}$ starting at M and finishing at infinity $\xi = i\infty + 0^-$ on the other side of the branch cut.

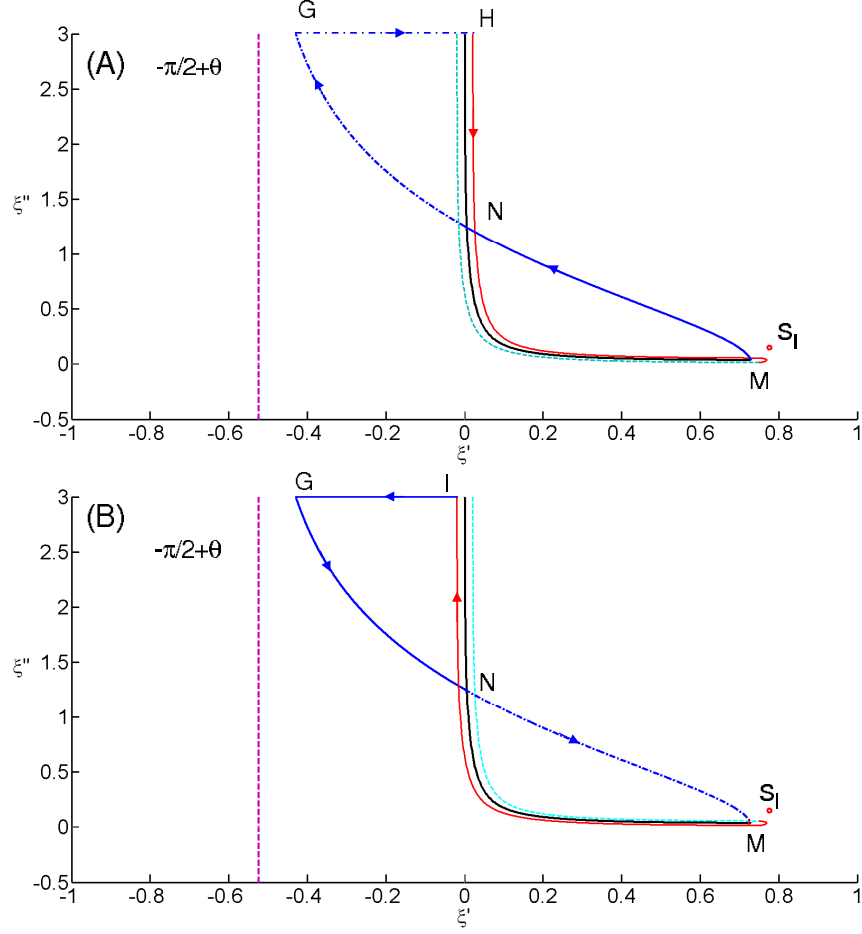


FIG. 3: Integration contour in the complex ξ -plane along the branch cut HI around the branch point M for $\vartheta > \xi'_c$. (A) shows the closed contour used to deform analytically the contour HM . (B) shows the closed contour used to deform the contour MI .

As shown in Fig. 3(A) in order to calculate I_{HM} the integration contour is closed by longing the modified steepest descent path MG defined by the equation

$$\begin{aligned} \cos(\xi' - \vartheta) \cosh \xi'' &= \cos(\xi'_c - \vartheta) \cosh \xi''_c \\ &\simeq \cos(\vartheta_c - \vartheta) = K < 1. \end{aligned} \quad (39)$$

The curve MG with a vertical asymptote at $\xi = -\pi/2 + \vartheta$ is thus defined by $\xi'' = \text{arccosh}(K/\cos(\xi' - \vartheta))$. We thus have $0 = \int_{HM} + \int_{MN} + \tilde{\int}_{NG} + \tilde{\int}_{GH}$ where N is the intersection point between the modified steepest descent path MG and the branch cut ($\xi_N \simeq i \text{arccosh}(K/\cos(\vartheta))$). $\tilde{\int}_{NG} := \int_{NG} d\xi F_-(\xi) e^{ik_0 nr \cos(\xi - \vartheta)}$ and $\tilde{\int}_{GH} := \int_{GH} d\xi F_-(\xi) e^{ik_0 nr \cos(\xi - \vartheta)}$ are evaluated on the “-” Riemann sheet while $\int_{HM} := \int_{HM} d\xi F_+(\xi) e^{ik_0 nr \cos(\xi - \vartheta)}$ and $\int_{MN} := \int_{MN} d\xi F_+(\xi) e^{ik_0 nr \cos(\xi - \vartheta)}$ are evaluated on the “+” Riemann sheet. From H we cross a second time the branch cut in order to close the contour on the “+” Riemann sheet.

A similar analysis is done for the integration contour \int_{MI} . We have $0 = \int_{MI} + \int_{IG} + \int_{GN} + \tilde{\int}_{NM}$ where \int_{MI} , \int_{IG}

and \int_{GN} are defined as previously on the “+” Riemann sheet while $\tilde{\int}_{NM} := \int_{NM} d\xi F_-(\xi) e^{ik_0 nr \cos(\xi - \vartheta)}$ is evaluated on the “-” Riemann sheet. In order to close the contour in “+” we must finally cross the branch cut in the region surrounding M . The infinitesimal loop surrounding M gives however a vanishing contribution which can be neglected. Regrouping all these expressions we define $I_{LW} = -\int_{HM} - \int_{MI}$ and we obtain

$$I_{LW} = \int_{\xi_c}^{\xi_N} d\xi [F_+(\xi) - F_+(\xi)] e^{ik_0 nr \cos(\xi - \vartheta)} + \int_{\xi_N}^{-\pi/2 + \vartheta + i\infty} d\xi [F_-(\xi) - F_+(\xi)] e^{ik_0 nr \cos(\xi - \vartheta)} + \int_{IG} + \int_{GH}^{\sim}. \quad (40)$$

The contributions \int_{IG} , \int_{GH}^{\sim} vanish asymptotically as discussed before and therefore can be neglected. Importantly due to the definition of the square root the function $F_-(\xi) - F_+(\xi)$ tends to vanish at the intersection point N . We then define the function $\Phi(\xi) = [F_+(\xi) - F_+(\xi)] \text{sign}(\xi_N'' - \xi'')$ vanishing at ξ_c and write

$$I_{LW} = \Theta(\vartheta - \xi_c') \int_{\xi_c}^{-\pi/2 + \vartheta + i\infty} d\xi \Phi(\xi) e^{ik_0 nr \cos(\xi - \vartheta)}. \quad (41)$$

The Heaviside function was introduced in order to remember that I_{LW} is only defined if $\xi_c' < \vartheta$. In the present work we will only evaluate I_{LW} approximately using the method discussed in Ref. 2. First, we observe that $e^{ik_0 nr \cos(\xi - \vartheta)} = e^{ik_0 nr K} e^{k_0 nr \sin(\xi' - \vartheta) \sinh \xi''}$. Second, considering that only ξ values in the vicinity of $\xi_c \simeq \vartheta_c$ contribute significantly to I_{LW} we write $d\xi \approx i d\xi''$, and $\sin(\xi' - \vartheta) \sinh \xi'' \approx -\sin(\vartheta - \vartheta_c) \xi'' < 0$. We therefore obtain

$$\begin{aligned} I_{LW} &\approx i e^{ik_0 nr K} \Theta(\vartheta - \vartheta_c) \int_0^{+\infty} d\xi'' \Phi(\vartheta_c + i\xi'') e^{-k_0 nr \sin(\vartheta - \vartheta_c) \xi''} \\ &= 2i e^{ik_0 nr K} \Theta(\vartheta - \vartheta_c) \int_0^{+\infty} u du \Phi(\vartheta_c + iu^2) e^{-k_0 nr \sin(\vartheta - \vartheta_c) u^2} \end{aligned} \quad (42)$$

where we used the variable $\xi'' = u^2$. This integral is of the Gaussian kind and can be computed exactly using a Taylor expansion of Φ near ϑ_c . We consequently deduce

$$I_{LW} \approx i e^{ik_0 nr K} \Theta(\vartheta - \vartheta_c) \sum_{m=1}^{+\infty} \frac{\Gamma(1 + m/2)}{(k_0 nr \sin(\vartheta - \vartheta_c))^{1+m/2}} \frac{H^{(m)}(0)}{m!} \quad (43)$$

where we used the series expansion $\Phi(\vartheta_c + iu^2) = H(u) = \sum_{m=1}^{+\infty} \frac{u^m}{m!} \frac{d^m}{du^m} H(u)|_{u=0} = \sum_{m=1}^{+\infty} u^m \frac{H^{(m)}(0)}{m!}$ (the term $m = 0$ vanishes since $\Phi(\vartheta_c) = 0$).

The phase $\delta\varphi = k_0 nr \cos(\vartheta - \vartheta_c) = k_0 nr [\cos \vartheta \cos \vartheta_c + \sin \vartheta \sin \vartheta_c]$ takes a simple interpretation if you define the

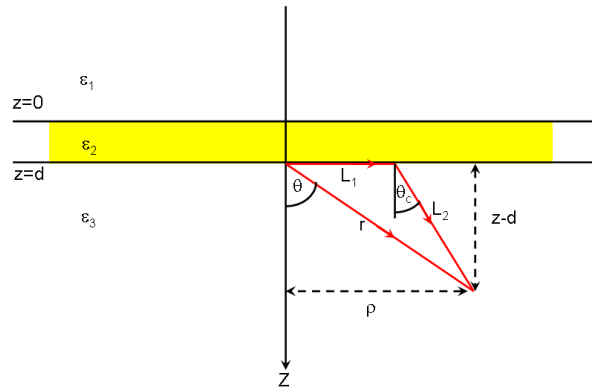


FIG. 4: Geometric construction of the Goos-Hänchen phase in transmission.

length L_1 of L_2 by:

$$\begin{aligned} r \sin \vartheta &= p = L_1 + L_2 \sin \vartheta_c \\ r \cos \vartheta &= z - d = L_2 \cos \vartheta_c. \end{aligned} \quad (44)$$

Therefore we obtain

$$\delta\varphi = k_0 n(L_2 + L_1 \sin \vartheta_c) = k_0 n L_2 + k_0 L_1 \quad (45)$$

where we used $n \sin \vartheta_c = 1$. As it is clear from Fig. 4 L_1 is the path length of a ‘creeping’ wave propagating along the interface before to be re-emitted at the critical angle ϑ_c . The re-emitted waves propagates along a distance L_2 in the medium of optical index n and then reaches the point defined by the coordinates (r, ϑ) . The phase $\delta\varphi$ is thus generated by a virtual propagation of length L_1 along the interface air-dielectric $z = d$ (supposing no metal is present and that the volume corresponding to the film between $z = 0$ and $z = d$ is filled with the medium of permittivity $\varepsilon_1 \simeq 1$) and followed by a re-emission at the critical angle in the glass substrate $\varepsilon_3 = n^2$. The previous analysis justifies therefore the name “lateral” we gave to the contribution I_{LW} . This effect can be seen as a kind of Goos-Hänchen deflection in transmission and is somehow equivalent to the already known Goos-Hänchen effect associated with lateral waves in the reflection mode.

E. The Far-field Fraunhofer regime

We are interested into evaluating the different integrals when $r \rightarrow +\infty$. As a first approximation, concerning I_{SDP} we calculate only the term $m = 0$ in the sum which reads:

$$I_{SDP,m=0} = \frac{\sqrt{\pi} e^{ik_0 n r}}{\sqrt{k_0 n r}} G(0) = \frac{\sqrt{2\pi} e^{ik_0 n r} e^{-i\pi/4}}{\sqrt{k_0 n r}} F_+(\vartheta). \quad (46)$$

In the far-field where $r \gg \lambda$ the Hankel function can be approximated using the asymptotic formulas

$$\begin{aligned} H_0^{(+)}(x) &= \sqrt{\frac{2}{\pi x}} e^{-i\pi/4} \left(1 - \frac{i}{8x}\right) e^{ix} + O(x^{-5/2}) \\ H_1^{(+)}(x) &= \sqrt{\frac{2}{\pi x}} e^{-i3\pi/4} \left(1 + \frac{3i}{8x}\right) e^{ix} + O(x^{-5/2}) \end{aligned} \quad (47)$$

which are valid for $x \gg 1$. Therefore for the vertical dipole we get

$$I_{SDP,m=0}^\perp = \frac{2\pi k_0 n \cos \vartheta}{ir} e^{ik_0 n r} \tilde{\Psi}^{\text{TM},\perp}[k_0 n \sin \vartheta \hat{\boldsymbol{\rho}}, z = d(1 - \frac{i}{8k_0 n r \sin^2 \vartheta} + \dots)] \quad (48)$$

where

$$\begin{aligned} \tilde{\Psi}_{\text{TM},\perp}[\mathbf{k}, z = d] &= \frac{i\mu_\perp}{8\pi^2 k_1} \tilde{T}_{13}^{\text{TM}}(k) e^{ik_3 d} e^{ik_1 h} \\ &= \frac{i\mu_\perp}{8\pi^2 k_0 \sqrt{(1 - n^2 \sin^2 \vartheta)}} \tilde{T}_{13}^{\text{TM}}(k) e^{ik_3 d} e^{ik_1 h} \end{aligned} \quad (49)$$

is the 2D Fourier transform of $\Psi^{\text{TM},\perp}(\varrho, z)$ calculated at $z = d$ (i.e $\int \frac{d^2 \mathbf{x}}{4\pi^2} \Psi^{\text{TM},\perp}(\varrho, z = d) e^{-i\mathbf{k} \cdot \mathbf{x}}$) for the wavevector $\mathbf{k} = k_0 n \sin \vartheta \hat{\boldsymbol{\rho}}$. Similarly for the Horizontal dipole we obtain for TM components:

$$I_{SDP,m=0}^\parallel = \frac{2\pi k_0 n \cos \vartheta}{ir} e^{ik_0 n r} \tilde{\Psi}^{\text{TM},\parallel}[k_0 n \sin \vartheta \hat{\boldsymbol{\rho}}, z = d] \left(1 + \frac{3i}{8k_0 n r \sin^2 \vartheta} + \dots\right) \quad (50)$$

where

$$\begin{aligned} \tilde{\Psi}^{\text{TM},\parallel}[\mathbf{k}, z = d] &= \frac{-i\mu_\parallel \cdot \mathbf{k}}{8\pi^2 k^2} \tilde{T}_{13}^{\text{TM}}(k) e^{ik_3 d} e^{ik_1 h} \\ &= \frac{-i\mu_\parallel \cdot \hat{\boldsymbol{\rho}}}{8\pi^2 k_0 n r \sin \vartheta} \tilde{T}_{13}^{\text{TM}}(k) e^{ik_3 d} e^{ik_1 h}. \end{aligned} \quad (51)$$

For TE components we have also:

$$I_{SDP,m=0}^{\parallel} = \frac{2\pi k_0 n \cos \vartheta}{ir} e^{ik_0 nr} \tilde{\Psi}^{\text{TE},\parallel} [k_0 n \sin \vartheta \hat{\boldsymbol{\rho}}, z = d] (1 + \frac{3i}{8k_0 nr \sin \vartheta^2} + \dots) \quad (52)$$

with now

$$\begin{aligned} \tilde{\Psi}^{\text{TE},\parallel} [\mathbf{k}, z = d] &= \frac{ik_0 \mu_{\parallel} \cdot (\hat{\mathbf{z}} \times \mathbf{k})}{8\pi^2 k_1 k^2} \tilde{T}_{13}^{\text{TE}}(k) e^{ik_3 d} e^{ik_1 h} \\ &= \frac{i\mu_{\parallel} \hat{\boldsymbol{\varphi}}}{8\pi^2 k_0 \sqrt{(1 - n^2 \sin^2 \vartheta^2)} n \sin \vartheta} \tilde{T}_{13}^{\text{TE}}(k) e^{ik_3 d} e^{ik_1 h}. \end{aligned} \quad (53)$$

In the far field only the term in $1/r$ survives and (in agreement with the Stratton-Chu formalism [3] and Richards and Wolf [4]) we can always write:

$$\begin{aligned} \Psi &\simeq I_{SDP,m=0} \simeq \frac{2\pi k_0 n \cos \vartheta}{ir} e^{ik_0 nr} \\ &\quad \tilde{\Psi}^{\text{TM or te}} [k_0 n \sin \vartheta \hat{\boldsymbol{\rho}}, z = d]. \end{aligned} \quad (54)$$

F. The intermediate regime: Generalization of the Norton wave

The next term in the power expansion of Ψ contributes proportionally to $1/r^2$. To evaluate this term we must take into account not only $I_{SDP,m=0}$ but also $I_{SDP,m=2}$ and $I_{LW,m=1}$. We use the notation

$$\begin{aligned} F_{\pm}(\xi) &= \sqrt{\left(\frac{2\pi k_0 n}{r}\right)} e^{-i\frac{\pi}{4}} k_0 n \cos \xi Q_{\pm}^{\alpha}(k_0 n \sin \xi) \\ &\quad \cdot [1 - i \frac{1 - 4\alpha^2}{k_0 nr (\sin \xi)^2} + \dots] \end{aligned} \quad (55)$$

(with $\alpha = 0$ or 1 depending whether the dipole is vertical or horizontal) and we obtain for the SDP contributions proportional to $1/r^2$:

$$I_{SDP,m=0} = \frac{2\pi(1 - 4\alpha^2)}{r^2} e^{ik_0 nr} \frac{\cos \vartheta Q_{+}^{\alpha}(k_0 n \sin \xi)}{(\sin \vartheta)^2} \quad (56)$$

and

$$\begin{aligned} I_{SDP,m=2} &= \frac{e^{ik_0 nr} \sqrt{\pi}}{4(k_0 nr)^{3/2}} \frac{d^2 G(\tau)}{d\tau^2} \Big|_{\tau=0} \\ &= \frac{-\pi}{r^2} e^{ik_0 nr} \frac{d^2 \left[\frac{\cos \xi}{\cos((\xi - \vartheta)/2)} Q_{+}^{\alpha}(k_0 n \sin \xi) \right]}{d\xi^2} \Big|_{\xi=\vartheta}. \end{aligned} \quad (57)$$

We also have to include the lateral wave (i.e. Goos-Hänchen) contribution:

$$I_{LW,m=1} \simeq e^{ik_0 nr K} \frac{i\sqrt{\pi} \Theta(\vartheta - \vartheta_c)}{2(k_0 nr \sin(\vartheta - \vartheta_c))^{3/2}} \frac{dH(u)}{du} \Big|_{u=0} \quad (58)$$

which reads

$$I_{LW,m=1} = \frac{\pi e^{ik_0(nL_2 + L_1)} \Theta(\vartheta - \vartheta_c) e^{i\frac{\pi}{4}}}{r^2 (\sin(\vartheta - \vartheta_c))^{3/2}} \frac{d\{\cos(\vartheta_c + iu^2) [Q_{+}^{\alpha}(k_0 n \sin(\vartheta_c + iu^2)) - Q_{-}^{\alpha}(k_0 n \sin(\vartheta_c + iu^2))]\}}{du} \Big|_{u=0}. \quad (59)$$

The sum $I_{SDP,m=0} + I_{SDP,m=2} + I_{LW,m=1}$ describes an asymptotic field varying as $1/r^2$ and which constitutes a generalization of the result obtained by Norton for the radio wave antenna on a conducting earth problem.

III. HOW TO DEFINE THE SURFACE PLASMON MODE?

A. From the near-field to the far-field

As seen in Section 2.E the dominant contribution in the far-field has the form

$$\Psi(\mathbf{x}, z) = \frac{2\pi k_0 n \cos \vartheta}{ir} e^{ik_0 n r} \tilde{\Psi}[k_0 n \sin \vartheta \hat{\boldsymbol{\rho}}, z = d]. \quad (60)$$

From Eq. 53 we also have the relation

$$\begin{aligned} \tilde{\Psi}[k_0 n \sin \vartheta \hat{\boldsymbol{\rho}}, z = d] &:= Q(s) \\ &= \sqrt{\left(\frac{r}{2\pi k_0 n}\right)} e^{i\frac{\pi}{4}} \frac{F_+(\xi)}{k_0 n \cos \xi} \\ &= \sqrt{\left(\frac{r}{2\pi k_0 n}\right)} e^{i\frac{\pi}{4}} F_+(\xi) \frac{d\xi}{ds} \end{aligned} \quad (61)$$

where $s = k_0 n \sin \xi$ and where ξ is here identical to ϑ (as usual the ϱ and φ dependencies are here implicit in $Q(s) := Q(s, \varphi, \varrho)$ and $F_+(\xi) := F_+(\xi, \varphi, \varrho)$). In the complex plane $\xi = \xi' + i\xi''$ and $s = s' + is''$ we have the singular/regular decomposition: $Q(s) = Q_0(s) + \text{Res}[Q(s_p)]/(s - s_p)$. Furthermore, from Eq. 59 this implies

$$\begin{aligned} \frac{1}{2\pi i} \oint_{C_p} ds Q(s) &= \text{Res}[Q(s_p)] \\ &= \sqrt{\left(\frac{r}{2\pi k_0 n}\right)} e^{i\frac{\pi}{4}} \frac{1}{2\pi i} \oint_{C_p} d\xi F_+(\xi) \\ &= \sqrt{\left(\frac{r}{2\pi k_0 n}\right)} e^{i\frac{\pi}{4}} \text{Res}[F_+(\xi_p)] \end{aligned} \quad (62)$$

where C_p and \mathcal{C}_p are small closed contours surrounding the plasmon pole in respectively the complex s -plane and ξ -plane. Therefore, we can equivalently write

$$Q(s) = Q_0(s) + \sqrt{\left(\frac{r}{2\pi k_0 n}\right)} e^{i\frac{\pi}{4}} \frac{\text{Res}[F_+(\xi_p)]}{s - s_p}. \quad (63)$$

The calculations being done in the far-field limit, where $r, \varrho \rightarrow +\infty$, we have for the vertical dipole case the residue:

$$\text{Res}[F_+^{\text{TM}, \perp}(\xi_p)] = \frac{i\mu_{\perp}}{8\pi} \frac{k_p}{k_{1,p}} e^{ik_{1,p}h} e^{ik_{3,p}d} \frac{N_{13}(k_p)}{\frac{\partial D_{13}(k_p)}{\partial k_p}} H_0^{(+)}(k_p \varrho) e^{-ik_p \varrho} \simeq \frac{i\mu_{\perp}}{8\pi} \frac{k_p}{k_{1,p}} e^{ik_{1,p}h} e^{ik_{3,p}d} \frac{N_{13}(k_p)}{\frac{\partial D_{13}(k_p)}{\partial k_p}} \sqrt{\left(\frac{2}{\pi k_p \varrho}\right)} e^{-i\frac{\pi}{4}}, \quad (64)$$

and similarly for the horizontal dipole residue:

$$\text{Res}[F_+^{\text{TM}, \parallel}(\xi_p)] = \frac{\boldsymbol{\mu}_{\parallel} \cdot \hat{\boldsymbol{\rho}}}{8\pi} e^{ik_{1,p}h} e^{ik_{3,p}d} \frac{N_{13}(k_p)}{\frac{\partial D_{13}(k_p)}{\partial k_p}} H_1^{(+)}(k_p \varrho) e^{-ik_p \varrho} \simeq \frac{\boldsymbol{\mu}_{\parallel} \cdot \hat{\boldsymbol{\rho}}}{8\pi} e^{ik_{1,p}h} e^{ik_{3,p}d} \frac{N_{13}(k_p)}{\frac{\partial D_{13}(k_p)}{\partial k_p}} \sqrt{\left(\frac{2}{\pi k_p \varrho}\right)} e^{-i\frac{3\pi}{4}}. \quad (65)$$

Regrouping all the terms and using the fact that $Q(s) = \tilde{\Psi}[\mathbf{k}, z = d]$ with $\mathbf{k} = k_0 n \sin \vartheta \hat{\boldsymbol{\rho}}$ and $\varrho = r \sin \vartheta$ this allow us to obtain a decomposition of the Fourier field $\tilde{\Psi}[\mathbf{k}, z = d]$ into a singular (i.e. SP) and regular contribution:

$$\tilde{\Psi}^{\perp, \parallel}[\mathbf{k}, z = d] = \tilde{\Psi}_0^{\perp, \parallel}[\mathbf{k}, z = d] + \tilde{\Psi}_{SP}^{\perp, \parallel}[\mathbf{k}, z = d] \quad (66)$$

with

$$\begin{aligned} \tilde{\Psi}_{SP}^{\perp}[\mathbf{k}, z = d] &= \frac{i\mu_{\perp}}{8\pi} \frac{k_p}{k_{1,p}} \frac{e^{ik_{1,p}h} e^{ik_{3,p}d}}{\pi \sqrt{k k_p} (k - k_p)} \frac{N_{13}(k_p)}{\frac{\partial D_{13}(k_p)}{\partial k_p}} \\ \tilde{\Psi}_{SP}^{\parallel}[\mathbf{k}, z = d] &= \frac{\boldsymbol{\mu}_{\parallel} \cdot \hat{\mathbf{k}}}{8\pi} \frac{e^{ik_{1,p}h} e^{ik_{3,p}d}}{i\pi \sqrt{k k_p} (k - k_p)} \frac{N_{13}(k_p)}{\frac{\partial D_{13}(k_p)}{\partial k_p}}. \end{aligned} \quad (67)$$

These formulas are rigorously only valid in the propagative sector where $|\mathbf{k}| \leq k_0 n$ (i.e. from the far-field definition). However, due to the simplicity of the mathematical expressions obtained one is free to extend the validity of Eqs. 65 to the full spectrum of $\mathbf{k} \in \mathbb{R}^2$ values including both the propagative sector for which $k_3 = \sqrt{(k_0^2 n^2 - |\mathbf{k}|^2)}$ and the evanescent sector for which $k_3 = i\sqrt{(|\mathbf{k}|^2 - k_0^2 n^2)}$ (i.e. if $|\mathbf{k}| \geq k_0 n$).

It should now be observed that we can slightly modify our current analysis by observing that Eq. 61 is not exactly a Laurent series since there are other isolated singularities in the complex plane which were here included in the definition of $Q_0(s)$ i.e. $\tilde{\Psi}_0^{\perp,||}[\mathbf{k}, z = d]$. The previous choice was justified for all practical purposes by the detailed calculation done in Section 2 in which only the ξ_p singularity corresponding to the s_l mode contributed to the integration contours used. Still, for the symmetry of the mathematical expressions it is clearly possible, and actually very useful (as we will see below), to extract a second SP contribution $\xi_{-p} = -\xi_p$ corresponding to $-k_p$. This is clearly the s_l pole associated with propagation in the opposite radial direction. Taking into account this second pole and the symmetries of k_{1p} , k_{3p} , $N_{13}(k_p)$ and antisymmetry of $\frac{\partial D_{13}(k_p)}{\partial k_p}$ in the substitution $k_p \rightarrow -k_p$ one obtain after straightforward calculations:

$$\begin{aligned}\tilde{\Psi}_{SP}^{\perp}[\mathbf{k}, z = d] &:= \frac{i\mu_{\perp}}{8\pi} \frac{k_p}{k_{1,p}} \frac{e^{ik_{1,p}h} e^{ik_{3,p}d}}{\pi\sqrt{k_p}} \frac{N_{13}(k_p)}{\frac{\partial D_{13}(k_p)}{\partial k_p}} \frac{1}{\sqrt{k}} \left[\frac{1}{k - k_p} + \frac{1}{i(k + k_p)} \right] \\ \tilde{\Psi}_{SP}^{||}[\mathbf{k}, z = d] &:= \frac{\boldsymbol{\mu}_{||} \cdot \hat{\mathbf{k}}}{8\pi} \frac{e^{ik_{1,p}h} e^{ik_{3,p}d}}{\pi\sqrt{k_p}} \frac{N_{13}(k_p)}{\frac{\partial D_{13}(k_p)}{\partial k_p}} \frac{1}{\sqrt{k}} \left[\frac{1}{i(k - k_p)} + \frac{1}{k + k_p} \right].\end{aligned}\quad (68)$$

From this definition we can calculate the SP field in the complete space. In particular for $z \geq d$ we have $\Psi_{SP}^{\perp,||}(\mathbf{x}, z) = \int d^2\mathbf{k} \tilde{\Psi}_{SP}^{\perp,||}[\mathbf{k}, z = d] e^{ik_3 Z}$ with $Z = z - d$. More precisely using the symmetry of the system we obtain

$$\begin{aligned}\Psi_{SP}^{\perp}(\mathbf{x}, z) &= \frac{i\mu_{\perp}}{8\pi} \frac{k_p}{k_{1,p}} \frac{e^{ik_{1,p}h} e^{ik_{3,p}d}}{\pi\sqrt{k_p}} \frac{N_{13}(k_p)}{\frac{\partial D_{13}(k_p)}{\partial k_p}} \\ &\cdot 2\pi \int_0^{+\infty} \frac{k dk e^{ik_3 Z} J_0(k\rho)}{\sqrt{k}} \left[\frac{1}{k - k_p} + \frac{1}{i(k + k_p)} \right]\end{aligned}\quad (69)$$

and

$$\begin{aligned}\Psi_{SP}^{||}(\mathbf{x}, z) &= \frac{\boldsymbol{\mu}_{||} \cdot \hat{\boldsymbol{\rho}}}{8\pi} \frac{e^{ik_{1,p}h} e^{ik_{3,p}d}}{\pi\sqrt{k_p}} \frac{N_{13}(k_p)}{\frac{\partial D_{13}(k_p)}{\partial k_p}} \\ &\cdot 2\pi \int_0^{+\infty} \frac{k dk e^{ik_3 Z} J_1(k\rho)}{\sqrt{k}} \left[\frac{1}{k - k_p} - \frac{1}{i(k + k_p)} \right].\end{aligned}\quad (70)$$

with $\mathbf{x} = \rho \hat{\boldsymbol{\rho}}$. To obtain these last equations we also used the well known Bessel function properties:

$$\begin{aligned}\oint d\varphi_k e^{ik\rho \cos(\varphi - \varphi_k)} \left\{ \begin{array}{c} \cos(m\varphi_k) \\ \sin(m\varphi_k) \end{array} \right\} \\ = 2\pi i^m \left\{ \begin{array}{c} \cos(m\varphi) \\ \sin(m\varphi) \end{array} \right\} J_m(k\rho)\end{aligned}\quad (71)$$

($m=0,1,\dots$) to integrate over the φ_k -coordinate of the 2D vector \mathbf{k} .

We point out that the convergence of integrals 69, 70 is ensured since the Cosine integral $\int_a^{+\infty} dk \cos(k\rho)/k = -\text{Ci}(a\rho) \simeq \frac{\cos(a\rho)}{(a\rho)^2} - \frac{\sin(a\rho)}{a\rho}$ for $a\rho \gg 1$ is bounded.

B. Asymptotic expansion

Remarkably, using the relations $H_0^{(+)}(u) - H_0^{(+)}(-u) = 2J_0(u)$ and $H_1^{(+)}(u) + H_1^{(+)}(-u) = 2J_1(u)$ (valid for $|\arg(z)| < \pi$) as well as the parity properties of the functions $\frac{1}{\sqrt{k}} \left[\frac{1}{k - k_p} \pm \frac{1}{i(k + k_p)} \right]$ (i.e. under the transformation

$k_p \rightarrow -k_p$) we obtain the practical relations

$$\begin{aligned} & \int_0^{+\infty} \frac{kdk e^{ik_3 Z} J_0(k\rho)}{\sqrt{k}} \left[\frac{1}{k-k_p} + \frac{1}{i(k+k_p)} \right] \\ &= \frac{1}{2} \int_{-\infty}^{+\infty} \frac{kdk e^{ik_3 Z} H_0^{(+)}(k\rho)}{\sqrt{k}} \left[\frac{1}{k-k_p} + \frac{1}{i(k+k_p)} \right] \end{aligned} \quad (72)$$

and

$$\begin{aligned} & \int_0^{+\infty} \frac{kdk e^{ik_3 Z} J_1(k\rho)}{\sqrt{k}} \left[\frac{1}{k-k_p} - \frac{1}{i(k+k_p)} \right] \\ &= \frac{1}{2} \int_{-\infty}^{+\infty} \frac{kdk e^{ik_3 Z} H_1^{(+)}(k\rho)}{\sqrt{k}} \left[\frac{1}{k-k_p} - \frac{1}{i(k+k_p)} \right]. \end{aligned} \quad (73)$$

Those relations would not be possible if we didn't included both the k_p and $-k_p$ poles in the analysis. Inserting Eqs. 72,73 into Eqs. 69,70 and using the complex variable ξ such as $k = k_0 n \sin \xi$ and the integration contour Γ used in the previous Sections we obtain

$$\Psi_{SP}^{\perp,||}(\mathbf{x}, z) = \int_{\Gamma} d\xi F_{SP}^{\perp,||}(\xi) e^{ik_0 n r \cos(\xi - \vartheta)} \quad (74)$$

where

$$\begin{aligned} F_{SP}^{\perp}(\xi) &= \frac{i\mu_{\perp}}{8\pi} \frac{k_p}{k_{1,p}} \frac{\sqrt{(k_0 n)} e^{ik_{1,p} h} e^{ik_{3,p} d}}{\sqrt{k_p}} \frac{N_{13}(k_p)}{\frac{\partial D_{13}(k_p)}{\partial k_p}} \frac{\sin \xi H_0^{+}(k_0 n \rho \sin \xi) e^{-ik_0 n \rho \sin \xi}}{\sqrt{\sin \xi}} \left[\frac{\cos \xi}{\sin \xi - \sin \xi_p} + \frac{\cos \xi}{i(\sin \xi + \sin \xi_p)} \right] \\ F_{SP}^{||}(\xi) &= \frac{\boldsymbol{\mu}_{||} \cdot \hat{\boldsymbol{\rho}}}{8\pi} \frac{\sqrt{(k_0 n)} e^{ik_{1,p} h} e^{ik_{3,p} d}}{\sqrt{k_p}} \frac{N_{13}(k_p)}{\frac{\partial D_{13}(k_p)}{\partial k_p}} \frac{\sin \xi H_1^{+}(k_0 n \rho \sin \xi) e^{-ik_0 n \rho \sin \xi}}{\sqrt{\sin \xi}} \left[\frac{\cos \xi}{\sin \xi - \sin \xi_p} - \frac{\cos \xi}{i(\sin \xi + \sin \xi_p)} \right]. \end{aligned} \quad (75)$$

The integral along Γ can be evaluated by using the same contour deformation as in Section 2. However, due to the absence of the square root k_1 in Eq. 75 there is no branch cut contribution to the integration contour. The integral can thus be split into one contribution from the residue and one contribution from the SDP. We get therefore:

$$\begin{aligned} \Psi_{SP}^{\perp,||}(\mathbf{x}, z) &= 2\pi i \text{Res}[F_{SP}^{\perp,||}(\xi_p)] e^{ik_0 n r \cos(\xi_p - \vartheta)} \Theta(\vartheta - \vartheta_{LR}) \\ &\quad + e^{ik_0 n r} \sum_{m \in \text{even}} \frac{\Gamma(\frac{m+1}{2})}{m!(k_0 n r)^{\frac{m+1}{2}}} \frac{d^m}{d\tau^m} G_{SP}^{\perp,||}(0) \end{aligned} \quad (76)$$

with $G_{SP}^{\perp,||}(\tau) = F_{SP}^{\perp,||}(\xi) \frac{d\xi}{d\tau}$.

Few remarks are here important:

(i) First, the singular term

$$2\pi i \text{Res}[F_{SP}^{\perp,||}(\xi_p)] e^{ik_0 n r \cos(\xi_p - \vartheta)} \Theta(\vartheta - \vartheta_{LR})$$

is exactly identical to the pole contribution appearing in Eq. 22. This results from the equality $\text{Res}[F_{SP}^{\perp,||}(\xi_p)] = \text{Res}[F_+^{\text{TM},\perp,||}(\xi_p)]$ (compare with Eqs. 24-25).

(ii) Second, the term $m = 0$ in the SDP contribution is dominant in the far-field regime and leads to $\Psi_{SP}^{\perp,||}(\mathbf{x}, z) = \frac{2\pi k_0 n \cos \vartheta}{ir} e^{ik_0 n r} \tilde{\Psi}_{SP}^{\perp,||}[k_0 n \sin \vartheta \hat{\boldsymbol{\rho}}, z = d]$ as expected.

(iii) Third, the decomposition $Q(s) = Q_0(s) + \text{Res}[Q(s_p)]/(s - s_p) + \text{Res}[Q(-s_p)]/(s + s_p)$ leads to

$$\begin{aligned} G_{SP}^{\perp,||}(\tau) &= G_{SP,0}^{\perp,||}(\tau) + \frac{\text{Res}[G_{SP}^{\perp,||}(\tau_p)]}{\tau - \tau_p} \\ &\quad + \frac{\text{Res}[G_{SP}^{\perp,||}(\tau_{-p})]}{\tau - \tau_{-p}} \end{aligned} \quad (77)$$

where $\tau_{-p} = -e^{i\pi/4}\sqrt{2}\sin((\xi_p + \vartheta)/2)$. Therefore, if we compare with Eqs. 32-38 we see that $\Psi_{SP}^{\perp,||}(\mathbf{x}, z)$ is not exactly equal to $I_{SP} + I_{SDP}^{\text{pole}}$ explicitly defined in Eqs. 37 and 36. More precisely we obtain:

$$\begin{aligned}\Psi_{SP}^{\perp,||}(\mathbf{x}, z) &= 2i\pi \text{Res}[G_{SP}^{\perp,||}(\tau_p)]e^{ik_0nr \cos(\xi_p - \vartheta)}\Theta(\vartheta - \vartheta_{LR}) \\ &\quad - e^{ik_0nr} \sum_{m \in \text{even}} \frac{\Gamma(\frac{m+1}{2})}{(k_0nr)^{\frac{m+1}{2}}} \frac{\text{Res}[G_{SP}^{\perp,||}(\tau_p)]}{\tau_p^{m+1}} \\ &\quad - e^{ik_0nr} \sum_{m \in \text{even}} \frac{\Gamma(\frac{m+1}{2})}{(k_0nr)^{\frac{m+1}{2}}} \frac{\text{Res}[G_{SP}^{\perp,||}(\tau_{-p})]}{\tau_{-p}^{m+1}} \\ &\quad + e^{ik_0nr} \sum_{m \in \text{even}} \frac{\Gamma(\frac{m+1}{2})}{m!(k_0nr)^{\frac{m+1}{2}}} \frac{d^m}{d\tau^m} G_{SP,0}^{\perp,||}(0)\end{aligned}\tag{78}$$

which differs from Eqs. 37, 38 by the two last lines. We can also rewrite these expressions as

$$\begin{aligned}\Psi_{SP}^{\perp,||}(\mathbf{x}, z) &= e^{ik_0nr} \sum_{m \in \text{even}} \frac{\Gamma(\frac{m+1}{2})}{m!(k_0nr)^{\frac{m+1}{2}}} \frac{d^m}{d\tau^m} G_{SP,0}^{\perp,||}(0) \\ &\quad + i\pi \text{Res}[G_{SP}^{\perp,||}(\tau_p)]e^{ik_0nr \cos(\xi_p - \vartheta)} \text{erfc}(-i\tau_p \sqrt{(k_0nr)}) \\ &\quad + i\pi \text{Res}[G_{SP}^{\perp,||}(\tau_{-p})]e^{ik_0nr \cos(\xi_p + \vartheta)} \text{erfc}(-i\tau_{-p} \sqrt{(k_0nr)})\end{aligned}\tag{79}$$

where we used Eq. 36. applied to τ_{-p} and τ_p .

IV. MORE ON INTENSITY AND FIELD IN THE BACK FOCAL PLANE AND IMAGE PLANE OF THE MICROSCOPE

A general analysis of the imaging process occurring through a microscope objective with high numerical aperture NA and an ocular tube lens is given in for example Ref. [5]. Here, we give without proofs the calculated field and intensity in the focal plane of the objective and the image plane of the microscope expressed in term of the TE and TM scalar potentials defined in Eqs. 1,2.

For this purpose we use the Fourier transform of the electromagnetic TM and TE field at the $z = d$ interface defined by:

$$\begin{aligned}\tilde{\mathbf{D}}_{\text{TM}}[\mathbf{k}, z] &= -\{\mathbf{k}k_3(k) - k^2\hat{\mathbf{z}}\}\tilde{\Psi}_{\text{TM}}[\mathbf{k}, z] \\ \tilde{\mathbf{D}}_{\text{TE}}[\mathbf{k}, z] &= -k_0n^2\mathbf{k} \times \hat{\mathbf{z}}\tilde{\Psi}_{\text{TE}}[\mathbf{k}, z].\end{aligned}\tag{80}$$

This implies [5] that the electric field recorded in the back focal plane of the objective is (i.e. taking into account the vectorial nature of the field and the transformation of the spherical wave front to a planar wave front):

$$\mathbf{E}_{\text{back focal plane } \Pi} = \frac{2\pi e^{ik_0nf}}{if} \frac{T_1 \sqrt{k_0k_3(k)}}{n} \{-k_0n\mathbf{k}\tilde{\Psi}_{\text{TM}}[\mathbf{k}, d] + k_0n^2k\hat{\varphi}_1\tilde{\Psi}_{\text{TE}}[\mathbf{k}, d]\}\tag{81}$$

with by definition $\hat{\varphi}_1 = -\mathbf{k} \times \hat{\mathbf{z}}/k$. The geometric coefficient $k_3(k)$ is reminiscent from the 'sin' condition [5] which lead to strong geometrical aberrations at very large angle θ . As a direct consequence we deduce the intensity in the back focal plane:

$$|\mathbf{E}_{\text{back focal plane } \Pi}|^2 = \frac{4\pi^2 t_1}{f^2 n^2} k_0k_3(k) [|\tilde{\mathbf{D}}_{\text{TM},3}[\mathbf{k}, d]|^2 + |\tilde{\mathbf{D}}_{\text{TE},3}[\mathbf{k}, d]|^2]\tag{82}$$

which is therefore proportional to the total Fourier field intensity for TM and TE waves taken separately. Finally, in the image plane we obtain the electric field :

$$\mathbf{E}(\mathbf{x}') = N' \int_{|\mathbf{k}| \leq k_0NA} d^2\mathbf{k} \sqrt{k_3(k)} e^{-i\mathbf{k} \cdot \frac{\mathbf{x}'}{M}} \cdot \{\tilde{\mathbf{D}}_{\text{TM},||}[\mathbf{k}, d] \frac{k_0n}{k_3(k)} + \tilde{\mathbf{D}}_{\text{TE}}[\mathbf{k}, d]\}\tag{83}$$

i.e.

$$\mathbf{E}(\mathbf{x}') = N' \int_{|\mathbf{k}| \leq k_0 NA} d^2 \mathbf{k} \sqrt{k_3(k)} e^{-i \mathbf{k} \cdot \frac{\mathbf{x}'}{M}} \cdot \{-k_0 n \mathbf{k} \tilde{\Psi}_{\text{TM}}[\mathbf{k}, d] + k_0 n^2 k \tilde{\varphi}_1 \tilde{\Psi}_{\text{TE}}[\mathbf{k}, d]\} \quad (84)$$

where N' is a constant characterizing the microscope. In the letter we used theses formulas for computing fields and intensity in the Fourier and image plane (see Figs. 3,4 of the letter).

Appendix A

We have by definition

$$\begin{aligned} \tau_p'' &= \sin((\xi_p' - \vartheta)/2) \cosh(\xi_p''/2) \\ &\quad + \cos((\xi_p' - \vartheta)/2) \sinh(\xi_p''/2). \end{aligned} \quad (A1)$$

The condition $\tau_p'' < 0$ is equivalent to $\tan((\xi_p' - \vartheta)/2) < -\tanh(\xi_p''/2)$, i.e. to

$$\begin{aligned} \frac{\xi_p' - \vartheta}{2} &< -\arctan(\tanh(\xi_p''/2)) \\ &= -\arccos\left(\frac{1}{\cosh(\xi_p'')}\right). \end{aligned} \quad (A2)$$

We therefore obtain $\vartheta_{LR} < \vartheta$ where holds the relation

$$\cos((\xi_p' - \vartheta_{LR}) \cosh \xi_p'') = 1. \quad (A3)$$

This is clearly the definition of the leakage radiation angle introduced in the discussion of the singular term I_{SP} . This therefore implies the equality

$$\Theta(\vartheta - \vartheta_{LR}) = \Theta(-\tau_p''). \quad (A4)$$

Appendix B

We have the relation $G(\tau) = F(\xi) \frac{d\xi}{d\tau}$ and we define

$$\begin{aligned} F(\xi) &= F_0(\xi) + \frac{\text{Res}[F(\xi_p)]}{\xi - \xi_p} \\ G(\tau) &= G_0(\tau) + \frac{\text{Res}[G(\tau_p)]}{\tau - \tau_p} \end{aligned} \quad (B1)$$

Therefore we obtain for the residues the relation:

$$\begin{aligned} \text{Res}[G(\tau_p)] &= \frac{1}{2\pi i} \oint_{C_p} d\tau G(\tau) \\ &= \frac{1}{2\pi i} \oint_{C_p} d\xi F(\xi) = \text{Res}[F(\xi_p)]. \end{aligned} \quad (B2)$$

-
- [1] R. E. Collin, IEEE Antennas and propagation magazine **46**, 64 (2004).
 - [2] L.M. Brekhovskikh, *Waves in Layered Media*, ch. 4 (Academic Press, 1960).
 - [3] J. A. Stratton and L. J. Chu, Phys. Rev **56**, 99 (1939).
 - [4] B. Richards and E. Wolf, Proc. Roy. Soc. London Ser. A **253**, 358, (1959).
 - [5] W. T. Tang, E. Chung, Y.-H. Kim, P. T. C. So and C. Sheppard, Opt. Express **15**, 4634 (2007).

Imaging surface plasmons: from leaky waves to far-field radiation

Aurélien Drezet

Institut Néel, UPR 2940, CNRS-Université Joseph Fourier, 25, rue des Martyrs, 38000 Grenoble, France

Cyriaque Genet

ISIS, UMR 7006, CNRS-Université de Strasbourg, 8, allée Monge, 67000 Strasbourg, France

(Dated: February 24, 2014)

We show that, contrary to the common wisdom, surface plasmon poles are not involved in the imaging process in leakage radiation microscopy. Identifying the leakage radiation modes directly from a transverse magnetic potential leads us to reconsider the surface plasmon field and unfold the non-plasmonic contribution to the image formation. While both contributions interfere in the imaging process, our analysis reveals that the reassessed plasmonic field embodies a pole mathematically similar to the usual surface plasmon pole. This removes a long-standing ambiguity associated with plasmonic signals in leakage radiation microscopy.

PACS numbers: 42.25.Lc, 42.70.-a, 73.20.Mf

Surface plasmon optics has become a mature and extended field of research, ranging from the development of new optical nanodevices and nanoantennas to the renewal of integrated quantum optics [1, 2]. In this context, surface plasmon imaging techniques are of critical importance to the researcher, among which leakage radiation microscopy (LRM) is now emerging as a powerful tool [3, 4]. As a far-field optical method, LRM is used for analyzing SP modes both in direct and Fourier (momentum) spaces and it has been successfully implemented in various plasmonic systems, both at the classical and quantum level [5–10]. Yet, there is still no satisfying theoretical definition of the SP field in an imaging context. Instead, recent reference work on leaky waves have focused on semi-infinite air-metal interfaces, a configuration not relevant to LRM [14–17]. This has fuelled recent debates concerning the precise relation between experimentally recorded images and SP modes [11–13].

In this Letter, we instead propose a novel approach to the problem of leaky waves that provides a full analytical theory of the coherent SP imaging process in the case of a point-like radiating electric dipole located in air above the thin metal film. This leads us to a new definition of the SP field as a Fano-type interfering component of the imaged radiation. We derive analytical expressions for the far-field radiation that meets all the necessary conditions prescribed to the leakage field symmetries [18]. Importantly, we show that our approach naturally makes the SP field free from the long standing ambiguities of the historical Zenneck and Sommerfeld solutions [19, 20] and removes the field discontinuity at the LR angle, until now problematic. Doing so, we also identify the contribution of a lateral wave thus far unnoticed that we associate with a new type of Goos-Hänchen effect in transmission.

In the geometry considered in Fig. 1, a harmonically radiating point-like dipole $\mu e^{-i\omega t}$ drives an SP wave that leaks through the film in medium 3 and then propagates in the matching oil of the high numerical aperture (NA)

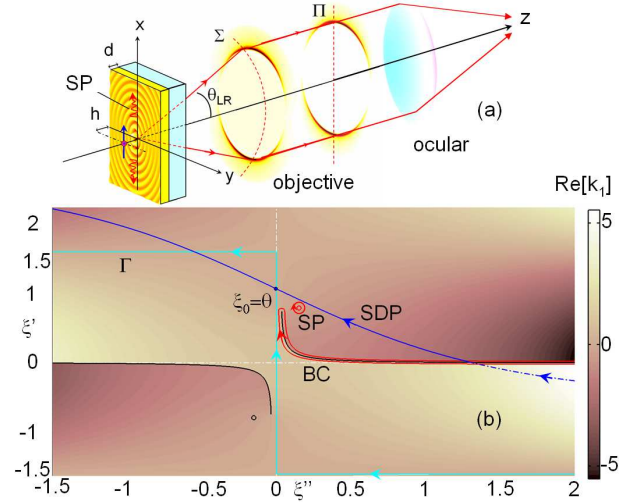


FIG. 1: (a) Sketch of the leakage radiation microscope: an electric dipole embedded in medium 1 with permittivity $\varepsilon_1 = 1$ (air) is located at $[x = 0, y = 0, z = -h]$ from the surface $z = 0$ of a thin (thickness d) metal film of permittivity ε_2 deposited on a glass substrate of permittivity $\varepsilon_3 = n^2 > \varepsilon_1$ (see [21]). (b) Integration path Γ in the $(\xi'' = \text{Im}(\xi), \xi' = \text{Re}(\xi))$ complex plane. BC is the branch-cut and SP the position of the plasmonic poles (symmetric leaky) in the two $\text{Im}(\xi) \cdot \text{Re}(\xi) > 0$ quadrants. The steepest descent path SDP is shown in the $\text{Im}(k_1) > 0$ first R_+ Riemann sheet (continuous line), and in the $\text{Im}(k_1) < 0$ second Riemann sheet (dot-dashed). The variations of $\text{Re}(k_1)$ are displayed with values given in the color-bar.

immersion objective required for LRM. Due to the specific dispersion relation of SP waves, leakage radiation (LR) is emitted at an angle $\vartheta_{LR} > \vartheta_c = \arcsin[\sqrt{\varepsilon_1/\varepsilon_3}]$ defining a radiation cone in the forbidden-light sector shown on Fig. 1(a) which intersects the reference sphere Σ of the LRM objective.

Due to the planar symmetry of the problem, the radiated field in medium 3 can be represented in terms of

transverse magnetic (TM) and electric (TE) scalar potentials Ψ with $[\nabla^2 + k_0^2 \varepsilon_3] \Psi_{\text{TM,TE}} = 0$ where $k_0 = \omega/c$. For simplicity, the case of a dipole normal to the film $\boldsymbol{\mu} = \mu_\perp \hat{\mathbf{z}}$ (i.e. $\Psi_{\text{TE}} = 0$) is only discussed here. A general and detailed calculation is given in [23]. Using boundary conditions at the different interfaces, we expand the potential at $[\mathbf{x} = (x, y), z]$ as $\Psi_{\text{TM}}(\mathbf{x}, z) = \int_{-\infty}^{+\infty} k dk A(k, z) H_0^{(+)}(k|\mathbf{x}|)$ with $A(k, z) = \frac{i\mu_\perp}{8\pi k_1} \tilde{T}_{13}^{\text{TM}}(k) e^{ik_1 z} e^{ik_3 z}$ and $H_0^{(+)}(k|\mathbf{x}|)$ is the zeroth order radiating-like Hankel function (evolving asymptotically as $e^{+ik|\mathbf{x}|}/\sqrt{k|\mathbf{x}|}$ for large $|\mathbf{x}|$). The Fresnel coefficient $\tilde{T}_{13}^{\text{TM}}(k)$ gives the transmission through the film of TM radiation with a wave vector $|\mathbf{k}| = k$. Stability imposes complex square roots $k_j(k) = \sqrt{k_0^2 \varepsilon_j - k^2}$ ($j = 1$ or 3) with $\text{Im}[k_j] \geq 0$.

The precise computation of such a Sommerfeld-like integral is extraordinarily involved due to the presence of two branch-cuts associated with $k_{1,3}(k)$ and several SP poles in the complex k -plane [24]. To simplify at most the problem, we chose an alternative parametrization of the integral through the complex variable ξ defining $k = k_0 n \sin \xi$. This leaves only one branch-cut $k_1 = k_0 \sqrt{\varepsilon_1 - \varepsilon_3 \sin^2 \xi}$ with a branch-point $\xi = \vartheta_c$. We impose $\text{Im}[k_1] \geq 0$ in the whole complex ξ -plane as the choice of the Riemann sheet R_+ . The integral becomes

$$\Psi_{\text{TM}}(\mathbf{x}, z) = \int_{\Gamma} d\xi F(\xi) e^{ik_0 n r \cos(\xi - \vartheta)} \quad (1)$$

where $F(\xi) = A(k, d) k k_3 H_0^{(+)}(k|\mathbf{x}|) e^{-ik|\mathbf{x}|}$ with the polar coordinates $|\mathbf{x}| = r \sin \vartheta$, $z = d + r \cos \vartheta$ leading to $(z - d) \cos \xi + |\mathbf{x}| \sin \xi = r \cos(\xi - \vartheta)$. The initial contour Γ corresponding to the condition $\sin \xi$ real is represented on Fig. 1(b).

To evaluate Eq. (1), we deform the contour Γ in order to include the steepest descent path (SDP) determined by $\text{Im}[f_\vartheta(\xi)] = 1$ with $f_\vartheta(\xi) = i \cos(\xi - \vartheta)$. The SDP crosses Γ at the saddle point $\xi_0 = \vartheta$ defined by $df(\xi)/d\xi = 0$. The SDP contribution Ψ_{SDP} to the field is calculated using the steepest-descent method discussed below. Two additional contributions Ψ_p and Ψ_{BC} associated respectively with the SP poles and the BC have to be accounted for when deforming the contour. The most relevant part here is a single SP pole $k_p = k_0 n \sin \xi_p$ resulting from the divergency of $\tilde{T}_{13}^{\text{TM}}(k) = \frac{N_{13}(k)}{D_{13}(k)}$ when $D_{13}(k_p) = 0$. Such a transcendental equation is known to possess four kinds of SP modes corresponding to leaky waves and bound modes in medium 1 or 3 [4, 18]. Importantly on the R_+ sheet, only the leaky mode in medium 3 (labeled symmetric leaky in [18]) is possibly encircled during the contour integration (see Fig. 1(b)) depending on whether $\xi_0 > \vartheta_{\text{LR}}$ or not. This implies that the residue contribution to Ψ_{TM} associated with the SP pole reads

$$\Psi_p = 2\pi i \text{Res}[F(\xi_p)] e^{ik_0 n r \cos(\xi_p - \vartheta)} \Theta(\vartheta - \vartheta_{\text{LR}}), \quad (2)$$

where $\Theta(x)$ is the Heaviside unit-step function and where the LR angle is precisely defined by $\text{Im}[f_{\vartheta_{\text{LR}}}(\xi_p)] = 1$, i.e. $\vartheta_{\text{LR}} = \text{Re}[\xi_p] + \arccos(1/\cosh \text{Im}[\xi_p]) \simeq \text{Re}[\xi_p]$. An in-

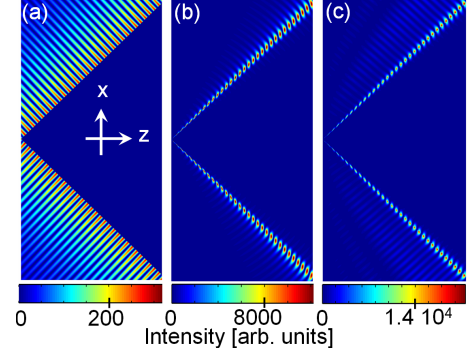


FIG. 2: Intensity contour-plots corresponding to the contributions (a) Ψ_p and (b) Ψ_{SDP} , with their coherent superposition displayed in (c). To remove the asymptotic divergence at infinity we calculated $|\mathbf{x}|(\text{Re}[\mathbf{E}])^2$ in (a), while we calculated instead $r^2(\text{Re}[\mathbf{E}])^2$ in (b, c).

tensity plot of this contribution is displayed on Fig. 2(a) which clearly shows the conical wave front structure emitted at the angle $\arctan(\text{Re}[k_p]/\text{Re}[k_{3p}]) = \text{Re}[\xi_p] \simeq \vartheta_{\text{LR}}$. Remarkably, this conical $\Theta(\vartheta - \vartheta_{\text{LR}})$ wave front removes the power flow divergence in the $z > 0$ direction due to the exponentially growing field associated with Ψ_p in medium 3 [18] and the spatial singularity along the z axis surviving at all distances away from the source induced by the Hankel function [23].

Beyond ϑ_{LR} , $\Psi_p \propto e^{ik_{3p} z} H_0^{(+)}(k_p |\mathbf{x}|)$ (where $k_{3p} := k_3(k_p)$) in direct relation to the original derivation by Zenneck and Sommerfeld of surface waves [19, 20]. It corresponds to what modern literature coined leaky SP mode [4, 18], belonging to the general family of leaky waves discussed for years in the radio antenna community [25]. It is important to realize however that this contribution is actually non-physical, due to the field discontinuity at ϑ_{LR} introduced by the $\Theta(\vartheta - \vartheta_{\text{LR}})$ pre-factor. It thus appears necessary to find a genuinely physical definition of a leaky SP wave. We now show that this is only possible by including in our discussion both Ψ_{SDP} and Ψ_{BC} contributions.

The central result of the Letter is that the LRM imaging process is essentially determined by Ψ_{SDP} which is evaluated as [23]

$$\Psi_{\text{SDP}} = e^{ik_0 n r} \sum_{m \in \text{even}} \frac{\Gamma(\frac{m+1}{2})}{m!(k_0 n r)^{\frac{m+1}{2}}} \frac{d^m}{d\tau^m} G(0) \quad (3)$$

with the variable $\tau = e^{i\pi/4} \sqrt{2} \sin((\xi - \vartheta)/2)$ and the function $G(\tau) = F(\xi) \frac{d\xi}{d\tau}$ in the vicinity of the saddle point $\tau = 0$ (i.e. $\xi_0 = \vartheta$). A second contribution must be accounted for when $\vartheta > \vartheta_c$ because in this case, the close integration path have to surround the branch-cut in the

R_+ sheet (see Fig. 1(b)). Following [26], this contribution can be given as a series expansion

$$\Psi_{BC} \approx e^{i\Delta\varphi} \Theta(\vartheta - \vartheta_c) \sum_{m=1}^{+\infty} \frac{\alpha_m(r, \vartheta_c)}{(k_0 n r \sin(\vartheta - \vartheta_c))^{1+m/2}} \quad (4)$$

where the coefficients $\alpha_m(r, \vartheta_c)$ can be explicitly computed and $\Delta\varphi = k_0 n r \cos(\vartheta - \vartheta_c)$ is interpreted as the phase accumulated by a wave creeping along the metal film (at velocity c) and re-emitted at the critical angle ϑ_c (at velocity c/n) [23]. Such a wave is associated in our case to a Goos-Hänchen-like effect in transmission [26]. This contribution is not specific to the LRM geometry but it has never been discussed whereas the $m = 1$ far-field dominant term in Eq. (4) evolves as $\sim 1/r^2$, i.e. as a Norton wave defined on the same $1/r^2$ order from Ψ_{SDP} [27].

These terms however can be neglected in the far field ($r \gg 2\pi/k_0$) where only survives the dominant $1/r$ term in the power expansion of $\Psi_{SDP, m=0}$ in Eq. (3). The radiated far field is thus

$$\Psi_{SDP, m=0}(\mathbf{x}, z) \simeq \frac{2\pi k_0 n \cos \vartheta}{i r} e^{ik_0 n r} \tilde{\Psi}_{TM}[\mathbf{k}, d] \quad (5)$$

where $\tilde{\Psi}_{TM}[\mathbf{k}, d] = A(k, d)/\pi$ is the bidimensional Fourier transform of $\Psi_{TM}(\mathbf{x}, z)$ calculated at $z = d$ for the in-plane wave vector $\mathbf{k} = k_0 n \sin \vartheta \mathbf{x}/|\mathbf{x}|$. This expression shows in Fig. 2(b) a conical structure peaked on ϑ_{LR} which should be compared with the one obtained from Ψ_p alone in Fig. 2(a). The comparison with Fig. 2(c) combining both contributions coherently clearly expresses a central result for LRM: $\Psi_{SDP, m=0}$ strongly dominates not only over Ψ_{BC} , as discussed above, but also over Ψ_p , consistently with the finite value of the SP propagation length $L_p = (2\text{Im}[k_p])^{-1}$ that overdamps the exponential tail of Ψ_p for angles $\vartheta \geq \vartheta_{LR}$.

From an imaging perspective, the radiating field given by Eq. (5) is detected in the objective back-focal plane Π sketched in Fig. 1 (see [21]). We plot $I_{TM, \Pi}[\mathbf{k}]$ in Fig. 3 for a dipole either perpendicular or parallel to the interface [28]. We point out that these intensity maps are in quantitative agreement with experiments [4, 8, 10] and clearly reveal a bidimensional ring with radius $k_r \approx \text{Re}[k_p]$ and width $\delta k \approx 2\text{Im}[k_p]$.

As a fundamental paradox, this ring is nowadays associated with the detection of the SP mode [4, 29, 30] despite the fact that it is Ψ_{SDP} and certainly not Ψ_p which is involved in the measurement process. This paradox stems from $G(\tau)$ being singular (thus Ψ_{SDP} too) at the SP pole τ_p (i.e. ξ_p), with a polar contribution Ψ_{SDP}^{pole} sharing a closed mathematical relation with Ψ_p . This generated an historical confusion regarding the actual role of SP modes in the Sommerfeld integral, an issue debated since the work of Zenneck and Sommerfeld [14, 19, 20].

In order to remove the ambiguity, we reconsider the very definition of what the SP field is, by going back to

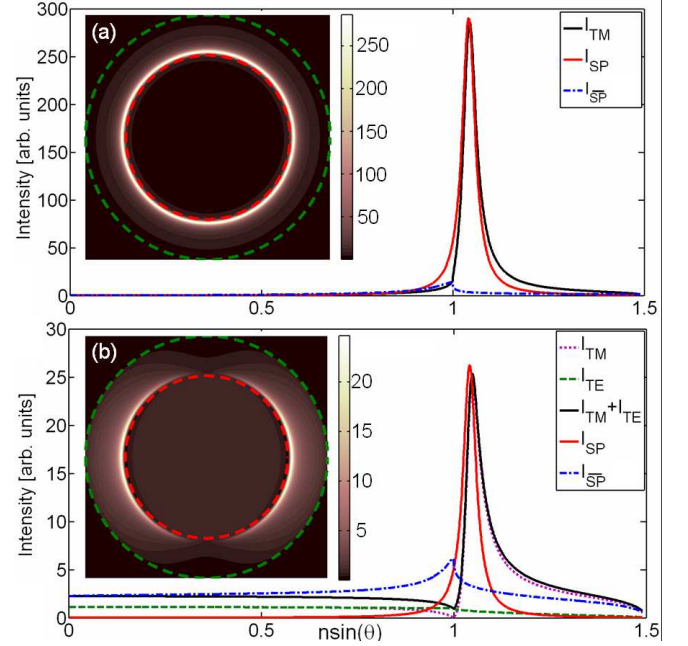


FIG. 3: Fourier space images recorded in the back-focal plane of the microscope objective for a dipole radiating through a thin metal film, when the dipole is perpendicular (a) or parallel (b) to the metal film. In both cases, the calculated accessible intensities in the $\mathbf{k} = [k_x, k_y]$ -plane $I_{TM, TE}$ are associated with $\tilde{\Psi}_{TM, TE}$ and I_{SP} with the SP contribution $\tilde{\Psi}_{SP}$. The non-plasmonic term $I_{\overline{SP}}$ is defined as a residual $\propto k_0^3 k_3 k^2 \varepsilon_3 |\tilde{\Psi}_{TM} - \tilde{\Psi}_{SP}|^2$ (a) and $\propto k_0^3 k_3 k^2 \varepsilon_3 |\tilde{\Psi}_{TM} - \tilde{\Psi}_{SP}|^2 + I_{TE}$ (b).

Eq. (3) and observing that $\tilde{\Psi}_{TM}[\mathbf{k}, d]$ is an explicit function of $k = k_0 n \sin \vartheta$ with $\vartheta \in [0, \pi/2]$. This function can be easily continued over the complex k -plane analytically. This function presents some isolated poles such as k_p and $-k_p$ which allow us to decompose $\tilde{\Psi}_{TM}[\mathbf{k}, d]$ into a regular and polar part. It is this polar part

$$\tilde{\Psi}_{TM}^{pole}[\mathbf{k}, d] = \eta_p \frac{1}{\sqrt{k}} \left[\frac{1}{k - k_p} + \frac{1}{i(k + k_p)} \right] \quad (6)$$

with $\eta_p = \frac{i\mu_{\perp}}{8\pi} \frac{k_p}{k_{1p}} \frac{e^{ik_{1p}d}}{\pi\sqrt{k_p}} \frac{e^{ik_{3p}d}}{\frac{\partial D_{13}(k_p)}{\partial k_p}} \frac{N_{13}(k_p)}{\frac{\partial D_{13}(k_p)}{\partial k_p}}$ that we will define as the SP field $\tilde{\Psi}_{SP}[\mathbf{k}, d] := \tilde{\Psi}_{TM}^{pole}[\mathbf{k}, d]$ (see [23] for the general case). To justify this definition, we point out that from Eq. (6) we deduce a SP field $\Psi_{SP}(\mathbf{x}, z) = \int d^2\mathbf{k} \tilde{\Psi}_{TM}^{pole}[\mathbf{k}, d] e^{i\mathbf{k}\cdot\mathbf{x}} e^{ik_3(z-d)}$ which, in analogy with Eq. (1), is alternatively defined by a contour integral over ξ along Γ

$$\Psi_{SP}(\mathbf{x}, z) = \int_{\Gamma} d\xi F_{SP}(\xi) e^{ik_0 n r \cos(\xi - \vartheta)} \quad (7)$$

where $F_{SP}(\xi) = \tilde{\Psi}_{TM}^{pole}[\mathbf{k}, d] k k_3 H_0^{(+)}(k|\mathbf{x}|) e^{-ik|\mathbf{x}|}$. The remarkable fact about Eq. (7) is that it can be evaluated by the procedures used for Eq. (1) without any branch cut, and split into one contribution from the residue and

another from the SDP:

$$\Psi_{\text{SP}}(\mathbf{x}, z) = 2\pi i \text{Res}[F_{\text{SP}}(\xi_p)] e^{ik_0 n r \cos(\xi_p - \vartheta)} \Theta(\vartheta - \vartheta_{\text{LR}}) + e^{ik_0 n r} \sum_{m \in \text{even}} \frac{\Gamma(\frac{m+1}{2})}{m!(k_0 n r)^{\frac{m+1}{2}}} \frac{d^m}{d\tau^m} G_{\text{SP}}(0) \quad (8)$$

with $G_{\text{SP}}(\tau) = F_{\text{SP}}(\xi) \frac{d\xi}{d\tau}$. Importantly, the residue term in Eq. (8) is identical to Ψ_p given that $\text{Res}[F_{\text{SP}}(\xi_p)] = \text{Res}[F(\xi_p)]$.

In the far field, the $m = 0$ term in the sum dominates and we have $\Psi_{\text{SP}}(\mathbf{x}, z) \simeq \frac{2\pi k_0 n \cos \vartheta}{ir} e^{ik_0 n r} \tilde{\Psi}_{\text{SP}}[\mathbf{k}, d]$. In Fig. 3 we compare this expression for Ψ_{SP} to Eq. (5) by computing the intensity in the back-focal plane. In the case of a vertical dipole -Fig. 3(a)- the SP term $I_{\text{SP},\Pi}[\mathbf{k}]$, proportional to $|\tilde{\Psi}_{\text{SP}}[\mathbf{k}, d]|^2$, is quasi-identical to $I_{\text{TM},\Pi}[\mathbf{k}]$. We define the non-plasmonic signal by $I_{\text{SP}} \propto |\tilde{\Psi}_{\text{TM}}[\mathbf{k}, d] - \tilde{\Psi}_{\text{SP}}[\mathbf{k}, d]|^2$. In the case of a horizontal dipole -Fig. 3(b)- there is also an additional TE contribution $I_{\text{TE},\Pi}[\mathbf{k}] \propto |\tilde{\Psi}_{\text{TE}}[\mathbf{k}, d]|^2$ to I_{SP} . The intensity dip observed for such a horizontal dipole is attributed to a Fano-type interference effect in the \mathbf{k} -space between the peaked SP contribution and the broad non-plasmonic signal made explicit by our analysis [31, 32].

In a last step, we calculate direct space images

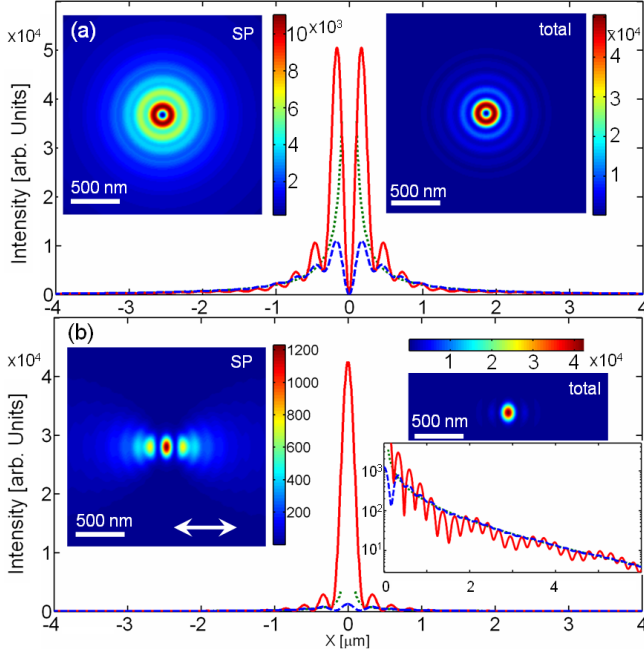


FIG. 4: Direct space images associated with a point-like dipole radiating through the metal film and recorded in the back focal plane of the microscope ocular. (a) Vertical dipole, (b) horizontal dipole (including in this case the additional TE contribution). The red curves correspond to the total signal computed from Eqs. (5) and (9) and the blue ones to the mere SP signal, i.e. Eqs. (8) and (9).

through a microscope ocular (see Fig. 1(a)) associated with SP propagation on the metal film by an inverse

Fourier transform of the field signal in the Π plane, taking into account the finite angular aperture of the objective [23]. We compare in Fig. 4 (a,b) the images calculated from Eqs. (5) and (8) respectively for a vertical and a horizontal dipole. Signal differences are more important for a horizontal dipole where TE and TM fields interfere, and decrease for distances larger than $2\pi/k_0$. We point out that the pure SP field at a point \mathbf{x}' of the image plane is given by a simple expression

$$\mathbf{E}_{\text{SP}}(\mathbf{x}') \propto \int_{|\mathbf{k}| \leq k_0 \text{NA}} d^2 \mathbf{k} \sqrt{k_3} \mathbf{k} \tilde{\Psi}_{\text{SP}}[\mathbf{k}, d] e^{i \frac{\mathbf{k} \cdot \mathbf{x}'}{M}} = - \int d^2 \mathbf{x} \mathbf{D}_{\text{SP},\parallel}(\mathbf{x}, d) \chi(\mathbf{x} + \frac{\mathbf{x}'}{M}) / \sqrt{k_{3p}} \quad (9)$$

where $\mathbf{D}_{\text{SP},\parallel}(\mathbf{x}, d) = \frac{\partial^2}{\partial \mathbf{x} \partial z} \Psi_{\text{SP}}(\mathbf{x}, d)$ is the in-plane component of the SP displacement field along the interface $z = d$ and $\chi(\mathbf{u}) \approx \frac{k_0 \text{NA}}{2\pi |\mathbf{u}|} J_1(k_0 \text{NA} |\mathbf{u}|)$ is the (scalar) point-spread function of the microscope objective. Taking a large microscope magnification $M = n f' / f \ll 1$ (with f, f' being respectively the objective and ocular focal lengths) enables us to analyze the recorded images simply using the paraxial-like Eq. (9), despite that leaky waves are emitted in a non-paraxial regime at ϑ_{LR} . Additionally, since $\tilde{\Psi}_{\text{SP}}[\mathbf{k}, d]$ defines a sharp ring-like distribution, we can approximately write $\mathbf{E}_{\text{SP}}(\mathbf{x}') \propto \mathbf{D}_{\text{SP},\parallel}(-\mathbf{x}'/M, d)$ for large $|\mathbf{x}'|/M$. Therefore, as shown in Fig. 4, the difference between the real image and the SP field vanishes asymptotically when $|\mathbf{x}'|$ increases. Finally, this analysis shows that only in-plane components of the SP field participate to the image, therefore resolving definitively the current controversy [11–13].

To conclude, we have removed the long-standing ambiguity associated with the very definition of a SP mode as probed in LRM through a revision of the SP field. We have shown how this field interferes, in a Fano-type way, with a broad non-plasmonic radiative signal in the LR imaging process. We expect our findings to have important impact in the ever-growing field of plasmonics in its different variants: classical to quantum through molecular to non-linear plasmonics.

This work was supported by Agence Nationale de la Recherche (ANR), France, through the PLASTIPS project and by the french program Investiment d'Avenir (Equipex Union).

-
- [1] W. L. Barnes, A. Dereux, and T. W. Ebbesen, *Nature* **424**, 824 (2003).
 - [2] M. Agio, *Nanoscale* **4**, 692 (2012).
 - [3] B. Hecht, H. Bielefeldt, L. Novotny, Y. Inouye, and D. W. Pohl, *Phys. Rev. Lett.* **77**, 1889 (1996).
 - [4] A. Drezet, A. Hohenau, D. Koller, A. Stepanov, H. Ditlbacher, B. Steinberger, F. R. Aussenegg, A. Leitner, J. R. Krenn, *Mat. Sci. Eng. B* **149**, 220 (2008).

- [5] A. L. Baudrion *et al.*, Opt. Express **16**, 3420 (2008).
- [6] Y. Gorodetski, K. Y. Bliokh, B. Stein, C. Genet, N. Shitrit, V. Kleiner, E. Hasman, and T. W. Ebbesen Phys. Rev. Lett. **109**, 013901 (2012).
- [7] L. Li, T. Li, S. M. Wang, and S. N. Zhu, Phys. Rev. Lett. **110**, 046807 (2013).
- [8] P. Bharadwaj, A. Bouhelier, and L. Novotny, Phys. Rev. Lett. **106**, 226802 (2011).
- [9] A. Cuche, O. Mollet, A. Drezet, and S. Huant, Nano Lett. **10**, 4566 (2010).
- [10] O. Mollet, S. Huant, G. Dantelle, T. Gacoin, and A. Drezet Phys. Rev. B **86**, 045401 (2012).
- [11] J. Wang, C. Zhao, and J. Zhang, Opt. Lett. **35**, 1944 (2010).
- [12] L. G. de Peralta, Opt. Lett. **36**, 2516 (2010).
- [13] A. Hohenau, J. R. Krenn, A. Drezet, O. Mollet, S. Huant, C. Genet, B. Stein, T. W. Ebbesen, Opt. Express **19**, 25749 (2011).
- [14] R. E. Collin, IEEE Ant. Prop. Magazine **46**, 64 (2004).
- [15] A. Yu Nikitin, S. G. Rodrigo, F. J. García-Vidal, and L. Martín-Moreno, New J. Phys. **11**, 123020 (2009).
- [16] P. Lalanne, J. P. Hugonin, H. T. Liu, and B. Wang, Surf. Sci. Rep. **64**, 453 (2009).
- [17] A. Yu Nikitin, F. J. García-Vidal, and L. Martín-Moreno, Phys. Rev. Lett. **105**, 073902 (2010).
- [18] J. J. Burke, G. I. Stegeman, and T. Tamir, Phys. Rev. B **33**, 5186 (1986).
- [19] J. Zenneck, Ann. Phys. **328**, 846 (1907).
- [20] A. N. Sommerfeld, Ann. Phys. **333**, 665 (1909).
- [21] We model the high NA aplanatic immersion LRM objective by a reference sphere Σ centered on $[x = 0, y = 0, z = 0]$ and of radius equal to the objective focal length f . The spherical wave front is transformed into a planar wave front Π at the back focal plane of the objective and converges, after an ocular of focal f' , in the image plane Π' . Note that since $\tan \vartheta_{LR} \geq 1$, non paraxial aberrations occurring during the propagation from Σ to Π have to be accounted for [22].
- [22] W. T. Tang, E. Chung, Y.-H. Kim, P. T. C. So and C. Sheppard, Opt. Express **15**, 4634 (2007).
- [23] See supplementary material linked at: <http://link.aps.org/supplemental/XXXXX> for mathematical details.
- [24] The additional branch-cut implied in principle by the $1/\sqrt{k|\mathbf{x}|}$ term of the Hankel function can be chosen running just below the Γ path with therefore no influence on further contour evaluations.
- [25] D. R. Jackson and A. A. Oliner, *Modern Antenna Handbook*, ch. 7 (C.A. Balanis Ed., Wiley, 2008).
- [26] L. M. Brekhovskikh, *Waves in Layered Media*, ch. 4 (Academic Press, 1960).
- [27] K. A. Norton, Proc. IRE **24**, 1367 (1936).
- [28] As shown in Fig. 3 vertical dipoles radiate typically ten times more light than in plane dipoles, meaning (in agreement with experiments [9, 22]) that the signal will be in general strongly dominated by vertical dipoles (see however [3, 13]).
- [29] L. Novotny, B. Hecht and D. Pohl J. Appl. Phys. **81**, 1798 (1997).
- [30] R. Marty, C. Girard, A. Arbouet, G. Colas des Francs, Chem. Phys. Lett. **532**, 100 (2012)
- [31] M. Sarrazin, J. P. Vigneron, and J.-M. Vigoureux, Phys. Rev. B **67**, 085415 (2003).
- [32] C. Genet, M.P. van Exter, J.P. Woerdman, Opt. Commun. **225**, 331 (2003).